Zebrafish (*Danio rerio*) aquaporin 1a as a multi-functional transporter of water, CO_2, and ammonia

By Krystle Talbot

January 6th, 2014

Thesis submitted to the
Faculty of Graduate and Postdoctoral Studies
University of Ottawa
in partial fulfillment of the requirements for the
MSc Degree in the
Ottawa-Carleton Institute of Biology

Thèse soumise à
l'Ecole d'études superieure et de recherché
Université d'Ottawa
envers la réalization partielle des éxigeances du degrée M.Sc.
de l'Institut de Biologie Ottawa-Carleton

ABSTRACT

Previous *in vitro* studies have demonstrated that AQP1, traditionally viewed as a water channel, also facilitates the passage of CO_2 and ammonia across cell membranes. This thesis summarizes the first *in vivo* studies confirming a physiologically-relevant role for AQP1 in acid-base balance and nitrogenous waste excretion. Zebrafish embryos were microinjected with a translation-blocking morpholino oligonucleotide targeted to the zebrafish AQP1 paralog, AQP1a. Closed-system respirometry, total CO_2 analysis, tritiated water fluxes and measurement of ammonia excretion were performed on larvae at 4 days post-fertilization (dpf). Knockdown of AQP1a significantly reduced rates of water, CO_2 and ammonia excretion. Use of phenylhydrazine, a haemolytic agent, provided evidence that the yolk sac epithelium AQP1a (and not erythrocyte AQP1a) is the major site of CO_2 and ammonia movements. Further, the hypothesis that AQP1a and the Rh glycoprotein Rhcg1, another multi-functional gas channel, act in concert to regulate CO_2 and ammonia excretion was explored. Exposure to conditions impairing ammonia excretion (such as high external ammonia (HEA) or alkaline water) modulated AQP1a protein expression in 4 dpf zebrafish larvae experiencing knockdown of Rhcg1. Chronic HEA exposure triggered a significant compensatory increase in AQP1a protein abundance in Rhcg1 morphants. Exposure of Rhcg1 morphants to pH 10 water, however, caused a significant decrease in AQP1a protein expression. Interestingly, when AQP1a mRNA and protein levels were examined in Rhcg1 morphants and vice versa, no changes were observed. Overall, zebrafish AQP1a was found to be a multi-functional transporter of water, CO_2 and ammonia, though the exact relationship it holds with other such gas channels bears further exploration.

RÉSUMÉ

Des études *in vitro* antérieures ont démontrées qu'AQP1, autrefois vu comme un canal pour l'eau, peut aussi faciliter le passage du CO_2 et de l'ammoniac à travers les membranes cellulaires. Cette thèse résume les premières études *in vivo* confirmant le rôle physiologiquement important de l'AQP1 dans le métabolisme acido-basique et l'excrétion de déchets azotés. Des embryons de poissons zèbre ont été micro-injectés avec un morpholino ciblant le blocage de la traduction d'un paralogue d'AQP1 chez les poissons zèbre, l'AQP1a. La réspirométrie en système fermé, l'analyse de CO_2 total, les flux d'eau tritié et les mesures d'excrétion d'ammoniac on été effectués sur des larves à 4 jours post-fertilisation (jpf). Le '' knockdown'' d'AQP1a a réduit les taux d'excrétion d'eau, de CO_2 et d'ammoniac de façon significative. L'utilisation de phénylhydrazine, un agent hémolytique, a fourni des preuves que l'AQP1a trouvé sur l'épithélium de la vésicule vitelline (plutôt que l'AQP1a des érythrocytes) est un site important de mouvement pour le CO_2 et l'eau. De plus, l'hypothèse que l'AQP1a et la glycoprotéine RH Rhcg1, un autre canal à gaz multifonctionnel, agissent ensemble afin de réguler l'excrétion d'eau et d'ammoniac a été explorée. Des conditions d'exposition atténuant l'excrétion d'ammoniac (telles que des concentrations élevées d'ammoniac externe (CEAE) ou de l'eau alkaline) ont modulé l'expression protéinique d'AQP1a chez les poissons zébre à 4 jpf sujet à un ''knockdown'' de Rhcg1. L'exposition chronique des morphants Rhcg1 à des CEAE a déclenché une augmentation compensatoire dans l'abondance protéinique d'AQP1a de façon significative. Cependant, l'exposition de morphants Rhcg1 à de l'eau à pH 10 a causé une diminution significative de l'expression protéinique d'AQP1a. Il est intéressant de noter que, lorsque les niveaux d'ARNm et protéine d'AQP1a furent examinés chez les morphants Rhcg1 et vice versa, aucuns changements ont été observés. Somme toute, l'AQP1a des poissons zèbres a été jugé comme étant un transporteur multifonctionnel d'eau, de CO_2 et d'ammoniac, quoique le lien entre l'AQP1a et d'autres canaux à gaz nécessite davantage de recherche.

ACKNOWLEDGEMENTS

First and foremost, I need to express my gratitude to Dr. Steve Perry and Dr. Kathleen Gilmour. I came into this M.Sc. with a varied background in molecular biology, chemistry, and biological engineering; their guidance and support eased the transition into the comparative physiology world and I haven't looked back since. Thank you for your seemingly infinite patience with me and calm encouragement. I thank the other members of my advisory committee, Dr. Pat Walsh and Dr. Tom Moon, for their many valuable insights and suggestions.

Secondly, I'd like to thank all past and present members of the Perry/Gilmour labs for their solid advice and friendship. I'd especially like to thank JB for being my mentor in the early days of this M.Sc. – she was there for me during times of uncertainty with kind words and expert technical assistance. I also need to thank RK for his patience in teaching me the trickier aspects of confocal microscropy. Last but not least, I thank VT for her wise words, laughter, and successful attempts at breaking me out of my introverted bubble. I wish you all the very best.

Thirdly, I thank my family for their love and unconditional support over these last two years. I cannot express how necessary you were to me during this time of personal and academic growth. To BM -- I couldn't have done it without you by my side.

Lastly, I acknowledge financial support from the University of Ottawa in the form of an admission scholarship. This research was funded in part by Natural Sciences and Engineering Research Council (NSERC) of Canada Discovery grants to SFP and KMG.

TABLE OF CONTENTS

LIST OF FIGURES

LIST OF ABBREVIATIONS

Abbreviation	Full name
Δ	Delta
°C	Degrees Celsius
Å	Ångstroms
µg	Microgram
µl	Microlitre
µM	Micromolar
µmol	Micromoles
µCi	Microcurie
^3H_2O	Tritiated water
ANOVA	Analysis of variance
ar/R	Aromatic arginine construction
AQP	Aquaporin
AQP1a	Zebrafish aquaporin 1a
BCA	Bichinchoninic acid
BSA	Bovine serum albumin
CA	Carbonic anhydrase
$CaCl_2$	Calcium chloride
cDNA	Complementary deoxyribonucleic acid
CO_2	Carbon dioxide
dpf	Days post-fertilization
DNA	Deoxyribonucleic acid
EDTA	Ethylenediaminetetraacetic acid
g	Gram
h	Hour
H^+	Hydrogen ion
HCO_3^-	Bicarbonate ion
HEA	High external ammonia
HEPES	4-(2-hydroxyethyl)-1-piperazineethanesulfonic acid
$HgCl_2$	Mercuric chloride
H_2O_2	Hydrogen peroxide
hpf	Hours post-fertilization
HR cell	H+ ATPase-rich cell
HRP	Horseradish peroxidase
IgG	Immunoglobulin G
J_{amm}	Rate of ammonia excretion
K_2CO_3	Potassium carbonate
kDa	Kilodaltons
KF	Potassium fluoride
L	Litre
$\dot{M}CO_2$	Rate of carbon dioxide excretion
mg	Milligrams

$MgSO_4$	Magnesium sulfate
min	Minutes
ml	Millilitre
mm	Millimetre
mM	Millimolar
mm Hg	Millimetres of mercury
$\dot{M}O_2$	Rate of oxygen uptake
NaCl	Sodium chloride
NaR cell	Na^+/K^+ ATPase-rich cell
ng	Nanogram
NH_3	Molecular ammonia
NH_4^+	Ammonium ion
NH_4Cl	Ammonium chloride
nl	Nanolitre
NPA	Asparagine-proline-alanine amino acid motif
NTA	Nitrilotriacetic acid
O_2	Oxygen
OUC	Ornithine-urea cycle
PBS	Phosphate-buffered saline
PCA	Perchloric acid
PCMBS	*p*-chloromercuriphenylsulfonic acid
PCO_2	Partial pressure of carbon dioxide
pH_i	Intracellular pH
pH_s	Surface pH
PHZ	Phenylhydrazine
PO_2	Partial pressure of oxygen
PVDF	Polyvinylidene fluoride
RBC	Red blood cell
RER	Respiratory exchange ratio
Rh glycoprotein	Rhesus glycoprotein
Rhag	Rhesus-associated glycoprotein
Rhbg	Rhesus B glycoprotein
Rhcg1	Rhesus C glycoprotein 1
RIPA	Radioimmunoprecipitation assay buffer
RNA	Ribonucleic acid
RT-PCR	Reverse transcriptase-polymerase chain reaction
SDS	Sodium dodecyl sulfate
SDS-PAGE	Sodium dodecyl sulfate polyacrylamide gel electrophoresis
SEM	Standard error of the mean
Tris	Tris(hydroxymethyl)aminomethane
Tris-HCl	Ttris(hydroxymethyl)aminomethane hydrochloride
vol/vol	Volume by volume

1. GENERAL INTRODUCTION

In the last decade, models of the processes underlying the transfer of small gaseous molecules across biological membranes have been significantly revised (Wright and Wood, 2009; Boron, 2010). The passage of physiologically important gases such as O_2, CO_2 and ammonia across biological membranes was long thought to be the result of simple diffusion driven by partial pressure gradients. However, the revelation that certain membranes [such as the apical membranes of rabbit gastric glands and colonic crypt cells (Boron, 2010; Singh *et al*, 1995)], have no demonstrable gas permeability has lead researchers to examine other possibilities. While it is likely that passive diffusion explains the bulk movement of most gases across most membranes, recent evidence suggests that membrane channel proteins can exhibit gas selectivity. Members of two multigene families, the aquaporins and the rhesus (Rh) glycoproteins, are understood to be involved in movement of CO_2 and ammonia, respectively (Cooper and Boron, 1998; Nazih *et al*, 1998; Prasad *et al*, 1998; Wright and Wood, 2009; Braun *et al*, 2009a).

The notion that a single membrane channel can function as a conduit for multiple gas species is controversial. Thus, although it was recently shown that certain members of the Rh glycoprotein family are capable of conducting both CO_2 and amnmonia (Kustu and Inwood, 2006; Endeward *et al*, 2008; Musa-Aziz *et al*, 2009; Perry *et al*, 2010), studies contradicting these findings remain numerous (Ripoche *et al*, 2006; Cherif-Zahar *et al*, 2007). *In vivo* work assessing the role of gas channels in carbon dioxide and ammonia metabolism is infrequent and often lacking entirely, especially in teleost fish. The purpose of this study was to establish whether or not the aquaporins are a second class of multi-functional gas channels, using zebrafish (*Danio rerio*) larvae as a model system.

1.1 Gas exchange in developing zebrafish

1.1.1 CO_2 excretion

Carbon dioxide acts as a weak acid in aqueous solutions (95% of total CO_2 in water is in the form of HCO_3^-), and thus acid-base homeostasis in bodily fluids requires CO_2 to be excreted as a metabolic waste product. In adult fish, the principal site of CO_2 excretion is the gill; ~95% of CO_2 excretion at the gill is thought to occur *via* passive diffusion of molecular (gaseous) CO_2 (Perry, 1986). Carbonic anhydrase (CA) catalyzes the reversible reactions of CO_2 and water – reactions that are critical for the movement of CO_2 among blood, tissues, and water. Briefly, CA in RBCs catalyzes the hydration of CO_2 to load HCO_3^- into the blood at the tissues. At the gills, CA catalyzes the reverse process, dehydrating HCO_3^- to CO_2, which then diffuses across the gill epithelium into the water (Perry, 1986; Perry and Gilmour, 2006). It is estimated that less than 5% of total CO_2 excreted in adult fish is in the form of HCO_3^- (Cameron, 1976).

In larval fish however, elimination of CO_2 occurs across the body surface. Rombough (2002) observed that gills in developing zebrafish only began to be used significantly for O_2 exchange at 14 days-post-fertilization (dpf). Prior to this point, cutaneous gas exchange was sufficient to meet respiratory requirements. Similar considerations are likely to apply to exchange of CO_2, although there are currently few in-depth studies that have examined CO_2 excretion in zebrafish larvae. Gilmour *et al* (2009) assessed CO_2 excretion during early development in zebrafish in the context of CA expression. Using microrespirometry techniques similar to those used in the present study, they calculated rates of CO_2 excretion ($\dot{M}CO_2$) in zebrafish larvae for the first five days post-fertilization. To compare CO_2 excretion relative to O_2 uptake ($\dot{M}O_2$), Gilmour *et al* (2009) calculated respiratory exchange ratios ($RER = \dot{M}CO_2/\dot{M}O_2$). Prior to hatching, rates of O_2 uptake outpaced rates of CO_2 excretion, implying CO_2 retention in

the embryonic tissues. Some have attempted to link embryonic CO_2 retention to the early ureotely of teleosts (Braun *et al*, 2009a), or to storage as carbonate for bone formation (Pellegrino and Biltz, 1965), although Gilmour *et al* (2009) suggested that CO_2 retention was far in excess of that needed for ureotely. Post-hatch, *RER* values >1 occurred, indicating conditions that favoured CO_2 excretion (Gilmour *et al*, 2009). A specific cause of this enhancement in CO_2 excretion was not pinpointed; the involvement of a gas channel in the cutaneous excretion of CO_2 during early development was not considered. *In situ* hybridization studies in zebrafish larvae have shown that by 72 hours-post-fertilization (hpf), AQP1a is expressed in ion transporting cells (ionocytes) of the yolk sac epithelium (Chen *et al*, 2010), where it could play a role in the increased cutaneous excretion of CO_2 observed post-hatch.

1.1.2 Ammonia excretion

Note that throughout this thesis, *ammonia* will refer to total ammonia ($NH_3 + NH_4^+$), *NH_3* will refer only to molecular NH_3, and *NH_4^+* will refer only to the protonated form of NH_3. Most adult teleost fish are ammonotelic, thus excreting more than half (but often up to 90%) of their nitrogenous waste as ammonia across the gills. Some exceptions exist; certain embryonic and juvenile species (such as rainbow trout and Atlantic cod) have a functional ornithine-urea cycle (OUC) and are ureotelic (Wright *et al*, 1995; Chadwick and Wright, 1999). Generally however, the high solubility of NH_3 coupled with an "acid-trapping" mechanism at the gill boundary layer (resulting in the conversion of NH_3 into NH_4^+, thus maintaining a favourable outward NH_3 partial pressure gradient) provides a simple enough method for extrusion of harmful nitrogenous waste products across the gill (Wilkie, 2002; Shih *et al*, 2008). In developing teleosts, members of the Rh glycoprotein family were shown to play an important role in increasing the ammonia permeability of the plasma membrane, and thus, in whole-body ammonia excretion. Members of

the Rh glycoprotein family now known to be selective ammonia transporters are Rh-associated glycoprotein (Rhag), Rh B glycoprotein (Rhbg), and Rh C glycoprotein (Rhcg) (Nakada *et al*, 2007; Wright and Wood, 2009; Braun *et al*, 2009a).

Braun *et al* (2009a) demonstrated that as zebrafish developed, the level of urea excreted dropped from ~80% to 15% of total nitrogen excretion as larvae completed the shift from ureotely to the ammonotely characteristic of adult freshwater teleosts. Moreover, a significant jump in ammonia excretion rates was observed at 2-3 dpf (following hatching), and this correlated with an increase in the expression of all three ammonia transporters; Rhag, Rhbg, and Rhcg1 (Braun *et al*, 2009a). Knockdown of any one of these Rh glycoproteins significantly reduced ammonia excretion in zebrafish larvae, to approximately 50% of control values (Braun *et al*, 2009a).

In zebrafish larvae, most ammonia excretion occurs *via* the yolk sac epithelium (Shih *et al*, 2008). The expression of Rhcg1 was localized to a class of V-type H^+-ATPase-rich (HR) cells, where it plays a role in generating the acidic external layer necessary for the maintenance of an outwardly-directed NH_3 partial pressure gradient (Shih *et al*, 2008). Immunohistochemistry revealed that AQP1a also is expressed in HR cells as early as 4 dpf (Kwong *et al*, 2013). Thus, it is possible that AQP1a plays a role (perhaps even in synergy with Rhcg1) in the cutaneous excretion of ammonia from zebrafish larvae. AQP1a is neither the first nor the only aquaporin to be implicated in nitrogenous waste elimination; previous work in this area will be examined in detail later in this review.

1.2 Rh glycoproteins - the first class of multi-functional gas channels

Several *in vitro* studies demonstrated the potential for Rh glycoproteins to function as a pathway for CO_2 flux (Kustu and Inwood, 2006; Endeward *et al*, 2008; Musa-Aziz *et al*, 2009; Perry *et al*, 2010). Human RBCs lacking Rhag exhibited a significantly lower PCO_2 than normal red blood cells; the same study concluded that Rhag was likely responsible for up to 30% of CO_2 movement in these cells (Endeward *et al*, 2008). A similar study by Musa-Aziz *et al* (2009) over-expressed Rhag in *Xenopus* oocytes and found that permeability to both ammonia and CO_2 was increased. Finally, the related Rh1 protein was reported to be necessary for CO_2 uptake during photosynthesis in the green algae *Chlamydomonas reinhardtii* (Kustu and Inwood, 2006). Nevertheless, the role of Rh glycoproteins in CO_2 movement remains controversial. For example, the rates of CO_2 and ammonia flux across red cell "ghost" membranes studded with Rhag were not significantly different from those of naked red cell ghost membranes (Ripoche *et al*, 2006), contradicting the above findings.

Translational knockdown of Rh proteins in zebrafish larvae provided the first *in vivo* evidence dependably linking Rh proteins to CO_2 and ammonia movement (Perry *et al*, 2010). Knockdown of the epithelial Rh proteins Rhcg1 or Rhbg significantly decreased both ammonia efflux and *RER*. The reduction of *RER* in combined Rhbg/Rhcg1 morphant larvae was substantial – a ~50% reduction compared to sham-injected larvae. Based on the results of CO_2-ammonia competition experiments in adult zebrafish from the same study, it was proposed that CO_2 and ammonia do indeed move through a common pathway in zebrafish *in vivo* (Perry *et al*, 2010). Thus, it appears that members of the Rh protein family are among the first class of multi-functional gas channels to be described. Although Perry *et al* (2010) focused on Rh glycoproteins, it is possible that other membrane channels, including aquaporins, may also play a role in dual CO_2/ammonia movement.

1.3 Aquaporins – the next class of multi-functional gas channels?

1.3.1 AQP structure and function

The AQPs form a superfamily of small pore-forming integral membrane proteins that facilitate efficient permeation of water molecules across membranes (Agre *et al*, 1993; Tingaud-Sequeira *et al*, 2010; Cerdà and Finn, 2010). Most AQPs consist of a single polypeptide chain varying in length from 24-30 kDa, forming six transmembrane α-helices. AQP monomers tend to assemble in the membrane as homotetramers, with each monomer functioning as an independent water channel around a larger central pore (Verbavatz *et al*, 1993; Walz *et al*, 1997). It has been suggested that this central pore is a potential route through which physiologically important gases may diffuse (Wang *et al*, 2007).

The water pore itself contains two highly-conserved constriction sites which confer AQPs with their water selectivity and ability to exclude ions. The first and narrowest of these is the aromatic arginine (ar/R) constriction, which forms the extracellular pore mouth. In water-specific AQPs, the ar/R constriction is ~2.8 Å in diameter (roughly the size of a water molecule), and in aquaglyceroporins, it is slightly larger at ~3.4 Å (Wu and Beitz, 2007). The positively-charged arginine residue is actively involved in ion exclusion (including H^+ exclusion; Beitz *et al*, 2006). The second constriction point is the Asn-Pro-Ala (NPA) motif, and the asparagine residues present therein re-orient water molecules such that they may be funnelled through the remaining part of the aquaporin pore (de Groot and Grubmüller, 2005). Formation of hydrogen bonds between proteins of the AQP pore and the water molecule is critical for passage through the pore (Wu and Beitz, 2007).

To date, 13 AQP subfamilies (AQP0-12) have been identified in teleosts and further sub-divided into two classes; the water-selective AQPs (AQP0, -1, -2, -4, -5 and -6) and the aquaglyceroporins (AQP3, -7, -9 and -10), which in addition to water are also permeable to larger-diameter molecules such as glycerol, urea, and NH_3. Exceptions to these classes are AQP8 (which is permeable only to water and ammonia) and AQP11/12 ("unorthodox" intracellular AQPs with poorly-defined properties; Cerdà and Finn, 2010). In recent years, the solute permeability of certain teleost aquaporins has expanded further to include nitric oxide (Herrera *et al*, 2006), arsenic (Hamdi *et al*, 2009) and hydrogen peroxide (Marchisso *et al*, 2012).

1.3.2 CO_2 permeability of AQPs

Since the serendipitous discovery of AQPs by Peter Agre's lab in 1992 (for which he was awarded a Nobel prize), several AQPs have been shown to demonstrate CO_2 permeability; AQP0, -1, -4, -5, -6, and -9 all are confirmed CO_2 transporters. Perhaps the most studied AQP in relation to CO_2 transport *in vitro* is AQP1. An early study reported that *Xenopus* oocytes over-expressing AQP1 demonstrated enhanced CO_2 permeability compared to control oocytes (Nahkoul *et al*, 1998). In the same year, Prasad *et al* (1998) used a fluorometric assay to measure CO_2 entry into proteoliposomes studded with AQP1 purified from human red blood cells. Both water and CO_2 permeability were markedly enhanced (nearly four-fold compared to controls) in these AQP1 vesicles, and this effect was abolished after application of $HgCl_2$, an AQP inhibitor. Cooper and Boron (1998) demonstrated that expression of AQP1a in *Xenopus* oocytes increased the rate at which intracellular pH (pH_i) decreased owing to the reactions between CO_2 and water, and that treatment with mercury derivative *p*-chloromercuriphenylsulfonic acid (PCMBS) negated this apparent increase in CO_2 permeability.

There is some debate as to whether AQP1-mediated CO_2 transport is physiologically relevant (Yang *et al*, 2000; Cooper *et al*, 2002; Fang *et al*, 2002). Use of AQP1-knockout mice as a model to study CO_2 permeability in RBCs and lung could not confirm a role for AQP1 (Yang *et al*, 2000). However, it has been suggested that issues with the experimental conditions may have masked the contribution of AQP1 to CO_2 permeability in the previous study (Cooper *et al*, 2002). In plants, the physiological importance of AQP1 is evident; over-expression of tobacco plant AQP1 increased the net photosynthesis rate of the plants by ~1.5x (CO_2 is the substrate during photosynthetic carbon fixation; Uehlein *et al*, 2003). In mammals, AQP1 is expressed abundantly in the proximal tubule of the kidney. As the point of CO_2 entry across the apical membrane, AQP1 contributes to the acidification of the proximal tubule and the reabsorption of HCO_3^- (Boron, 2006). Currently, *in vivo* studies assessing the physiological impact of AQP1 function on gas homeostasis in fish are lacking; the research detailed in this thesis seeks to eliminate this gap.

1.3.3 Ammonia permeability of AQPs

Holm *et al* (2005) used *Xenopus* oocytes (which are characteristically low in ammonia permeability) in a voltage-clamp experiment to study the effects of several AQPs on ammonia transport (pH_i was used as a measure of ammonia permeability). These researchers found that AQP3, -8, and -9 were permeable to ammonia. In particular, AQP8 was shown to quickly and selectively transport ammonia and water (Jahn *et al*, 2004; Saparov *et al*, 2007), leading it to be categorized separately from the more "classical" AQPs and the aquaglyceroporins.

Although AQP1 is now accepted as a channel for CO_2, whether AQP1 also allows passage of other physiologically important gases, such as ammonia, remains an open question. In oocytes expressing AQP1, the increased rate of intracellular acidification following exposure

to 20 mM NH_3/NH_4^+ was attributed to increased ammonia permeability *via* AQP1 (Nakhoul *et al*, 2001). Musa-Aziz *et al* (2009) demonstrated that oocytes over-expressing human-derived AQP1 exhibited a greater change in maximal surface pH (pH_s; ΔpH_s is an index of ammonia influx) when exposed to high external ammonia than control, water-injected oocytes, indicating that AQP1 is capable of conducting ammonia.

1.3.4 Zebrafish AQP1

To date, 18 gene sequences that are related to four different AQP families have been identified in zebrafish (Tingaud-Sequeira *et al*, 2010). Following the teleost-specific whole-genome duplication event, AQP0, -1, -3, -9, and -10 were duplicated. The two genes encoding AQP1 paralogs are *aqp1a* and *aqp1b*. Of particular interest is AQP1a because it is one of two AQPs (the other being AQP12) that is expressed ubiquitously in all zebrafish tissues throughout all stages of development. In contrast, AQP1b is expressed only in the brain, testis, and ovary (Tingaud-Sequeira *et al*, 2010). It has been speculated that AQP1b plays a role in maintaining egg hydration in marine oocytes and early embryos, ensuring their survival in the ocean (Tingaud-Sequeira *et al*, 2007), but it is unlikely to contribute significantly to gas homeostasis in freshwater zebrafish larvae. *In situ* hybridization studies (Chen *et al*, 2010) demonstrated that AQP1a in zebrafish is highly expressed in the vasculature and blood at 24 hpf but by 48 hpf, expression in the vasculature is reduced while it persists in the RBCs. After 72 hpf, AQP1a is expressed strongly in the swim bladder and ionocytes of the yolk sac epithelium. At least two sub-types of AQP1a-expressing ionocytes have been identified; the HR cells, and the Na^+/K^+-ATPase rich (NaR) cells (Kwong *et al*, 2013).

Based on the results of an *in vitro* study, Chen *et al* (2010) concluded that zebrafish AQP1a is indeed permeable to both CO_2 and ammonia. Given the abundant expression of

AQP1a on the yolk sac epithelium, the understanding that CO_2 and ammonia excretion both occur cutaneously during early larval development, and the abundance of evidence supporting AQP1 as a dual conduit for CO_2 and ammonia, it seemed reasonable to consider zebrafish AQP1a as an appropriate candidate for the first *in vivo* study of a multi-functional gas channel.

1.4 Model and hypotheses

1.4.1 Zebrafish as a model system

The choice of zebrafish as the organism for this study reflected their ease of breeding, short generation interval, and most importantly, their completely sequenced genome. Moreover, the well-established molecular biology techniques for this species permitted the translational knockdown of AQP1a and thus the *in vivo* assessment of its physiological function in larval zebrafish. Additionally, the previous *in vitro* work using zebrafish AQP1a (Chen *et al*, 2010) and the translational knockdown study of Rhcg1 in zebrafish larvae (Perry *et al*, 2010) form an appropriate context in which to consider the role of AQP1a in gas transfer *in vivo*.

1.4.2 Hypotheses

On the basis of previous *in vitro* work by Chen *et al* (2010) establishing zebrafish AQP1a as a transporter of CO_2 and ammonia, this thesis set out to test two hypotheses. First, it was hypothesized that AQP1a contributes to and may regulate CO_2 and ammonia excretion in larval zebrafish. Several predictions arise from this hypothesis. Functional knockdown of AQP1a would be predicted to reduce whole-body CO_2 excretion ($\dot{M}CO_2$), respiratory exchange ratio ($RER = \dot{M}CO_2/\dot{M}O_2$), and ammonia excretion (J_{amm}). Also, exposure to environmental conditions favouring ammonia loading into tissues (such as high external ammonia) would be predicted to increase AQP1a protein expression as a compensatory mechanism to excrete the

excess ammonia. Finally, exposure to conditions impeding ammonia excretion (such as high-pH water) would be predicted to trigger compensatory increases in AQP1a protein expression. Secondly, it was hypothesized that AQP1a and Rhcg1 (both shown to be multi-functional gas channels) act in concert to regulate CO_2 and ammonia movement across the larval body surface. Based on this hypothesis, knockdown of AQP1a in larvae would be predicted to trigger a compensatory increase in Rhcg1 mRNA and protein expression. Similarly, knockdown of Rhcg1 in larvae would be predicted to cause a compensatory increase in AQP1a mRNA and protein expression.

2. MATERIALS AND METHODS

2.1 Experimental animals

Adult zebrafish (*Danio rerio*) were purchased from Big Al's Aquarium Services (Ottawa, ON, Canada) and housed in the University of Ottawa's Aquatic Care Facility. The fish were held in tanks supplied with aerated, flowing, dechloraminated city of Ottawa tap water at 28°C, subjected to a constant 14-h:10-h light:dark photoperiod, and fed daily with No. 1 crumble-Zeigler (Aquatic Habitats, Apopka, FL). Embryos were obtained using standard breeding procedures (Westerfield, 1995), and were raised in 50 ml Petri dishes containing E3 medium (5 mM NaCl, 0.17 mM KCl, 10 mM HEPES, 0.33 mM $CaCl_2$, 0.33 mM $MgSO_4$, 0.0001% methylene blue) and held in incubators kept at 28°C. Dead embryos were removed and medium was refreshed daily. All analyses were performed at 4 days post fertilization (dpf) unless otherwise specified and therefore larvae were not fed for the duration of the experiments. All procedures were conducted in compliance with University of Ottawa institutional guidelines, were approved by the Animal Care Committee (protocol BL-226), and were in accordance with the guidelines of the Canadian Council on Animal Care for the use of animals in research and teaching.

2.2 Experimental protocols

Four experimental series were carried out. The goal of the first series was to determine whether functional knockdown of AQP1a affected CO_2 and/or ammonia excretion. In the second experimental series, phenylhydrazine treatment was used to eliminate RBCs to distinguish between contributions of AQP1a on RBCs and AQP1a on the yolk sac epithelium. The third experimental series explored the possibility of interactions between AQP1a and Rhcg1. Finally,

the contribution of AQP1a to CO_2 and ammonia excretion was assessed under conditions designed to impair ammonia excretion (high external ammonia or high pH).

2.2.1 Effects of AQP1a knockdown on CO_2 and ammonia excretion

2.2.1.1 Morpholino-based translational knockdown of AQP1a

A morpholino oligonucleotide (5′-AAG CCT TGC TCT TCA GCT CGT TCA T-3′; Genetools, OR, USA) was designed to be complementary to the translational start site of zebrafish AQP1a (GenBank ID: NM 207059.1). The morpholino was prepared to a final concentration of 4 ng nl^{-1} in 1X Danieau buffer [58 mM NaCl, 0.7 mM KCl, 0.4 mM $MgSO_4$, 0.6 mM $Ca(NO_3)_2$, 5.0 mM HEPES (pH 7.6)] with 0.05% (vol/vol) phenol red (as a visible indicator of successful injection). The morpholino was injected (4 ng $embryo^{-1}$) into embryos at the one- to two-cell stage using a microinjector system (model IM 300; Narishige, Long Island, NY) with injection needles pulled from 1.0-mm borosilicate glass (Sutter Instrument, Novata, CA, USA). To control for possible effects of microinjection, a "sham" group of embryos was injected with a standard (control) morpholino from GeneTools (5′-CCT CTT ACC TCA GTT ACA ATT TAT A-3′) at the same concentration. Both the control and AQP1a morpholinos were conjugated to a carboxyfluorescein molecule at the 3' end. Therefore, embryos were screened for fluorescence *in vivo* at 24 h post-injection to check for successful incorporation of the morpholino. Only embryos that exhibited widespread green fluorescence were raised to 4 dpf for experimentation. Neither obvious morphological deformities nor substantial mortality was observed following AQP1a knockdown.

2.2.1.2 Confirmation of AQP1a knockdown

To confirm successful knockdown of AQP1a, AQP1a protein levels were assessed by western blotting and immunohistochemistry, and *in vivo* water influx rates were assessed isotopically. Protein samples were isolated from pools of 20 larvae (N = 1) that were homogenized in RIPA buffer (150 mM NaCl, 1% Triton X-100, 0.5% sodium deoxycholate, 0.1% SDS, 50 mM Tris-HCl, 1 mM EDTA, 1 mM phenylmethanesulphonyl fluoride) containing a protease inhibitor cocktail (Roche, USA). Total protein concentration was assessed using the bichinchoninic acid (BCA; Sigma) technique (Smith, 1985), using bovine serum albumin (BSA) as the standard. Extracted protein was mixed 1:1 with Laemmli's sample buffer (Sigma-Aldrich, USA) and heated for 10 min at 65°C. Samples were size-fractionated on a 12% SDS-PAGE gel and then transferred *via* semi-dry Bio-Rad Trans-Blot SD transfer system to a polyvinylidene fluoride (PVDF) membrane (Bio-Rad, USA). Membranes were blocked for 1 h at room temperature with 5% skim milk powder in TBST (20 mM Tris, 300 mM NaCl, 0.1% Tween 20 containing 0.02% sodium azide, pH 7.5). Membranes were then probed overnight at 4°C using an anti-AQP1a antibody raised against a 15 amino acid residue in eel (*Anguilla anguilla*) AQP1a (custom polyclonal antibody raised against VNGPDDVPAVEMSSK; 87% identity with zebrafish AQP1a at the C-terminal; the antibody was a kind gift from Dr. Gordon Cramb); the antibody was used at a dilution of 1:1,000 in 2% skim milk/TBST. Following incubation with the primary antibody, membranes were washed with TBST (3 x 5 min) and incubated with a 1:5,000 dilution of horseradish-peroxidase (HRP) goat anti-rabbit IgG (Pierce, USA) for 2 h at room temperature. After a final wash in TBST (3 x 15 min), band detection was performed using Luminata Western HRP substrates (Millipore, USA). To control for protein loading, membranes were re-probed with a 1:1,000 dilution of anti-β-actin (A2066, Sigma-Aldrich, USA) following stripping of the membrane with Re-Blot Plus solution (Millipore, USA) used

according to the manufacturer's instructions. Quantification of band density was performed using ImageJ software (http://imagej.nih.gov/ij/), and AQP1a protein expression was normalized to that of β-actin.

Measurement of water influx rate was used as a second method of confirming successful knockdown of AQP1a. Groups of sham and AQP1a morphant larvae were exposed separately to 1 μCi ml^{-1} of ^3H_2O (American Radiolabeled Chemicals Inc., USA) for 4 h. Larvae were then euthanized by immersion in a solution of tricaine methanesulphonate (250 mg l^{-1}; Argent Chemical Laboratories, Redmond, WA), washed in isotope-free water, and pooled into groups of three as one sample (N = 1). Water samples (50 μl) were also collected at the beginning and end of the flux period to determine the specific activity of ^3H_2O. Fish samples were digested with a tissue solubilization reagent (80 μl; Solvable^{TM}; Perkin Elmer, USA) and neutralized with glacial acetic acid (~0.4 ml) before addition of scintillation cocktail (10 mL; BioSafe-II; RPI co. Mt. Prospect, IL, USA). Radioactivity of the digested fish and water samples was quantified using a liquid scintillation counter (LS-6500; Beckman Coulter Co., Canada). Influx of ^3H_2O was calculated by dividing the radioactivity of the fish (in counts per minute, cpm) by the specific activity of the water, number of fish, and duration of the experiment (in h).

Immunohistochemistry using the eel anti-AQP1a antibody was carried out as a qualitative method of confirming knockdown and to examine the localization of AQP1a in larvae. Larvae (sham and AQP1a morphants) were euthanized as described above and fixed for 2 h at room temperature in a solution of 4% paraformaldehyde prepared in phosphate-buffered saline (PBS; 137 mM NaCl, 2.7 mM KCl, 10 mM Na_2HPO_4, 1.8 mM KH_2PO_4). Following fixation, samples were washed with PBST (PBS containing 0.8% Triton-X) and heated for 10 min at 65°C in 150 mM Tris buffer (pH 9) to improve antigen retrieval. Samples were washed again in PBST and

blocked for 1 h at room temperature in PBST containing 10% goat serum (Jackson ImmunoResearch, USA). Samples were then incubated at 4°C overnight with the AQP1a antibody (1:250 dilution), also in 10% goat serum. Subsequently, samples were incubated in the dark with an Alexa 488-conjugated goat anti-rabbit IgG (Invitrogen) at 1:500 dilution for 2 h at room temperature. Samples were examined using an A1R+ A1+ Nikon confocal microscope (Nikon Instruments, USA).

2.2.1.3 Measurement of CO_2 and ammonia excretion in AQP1a morphants

Rates of O_2 consumption ($\dot{M}O_2$), CO_2 excretion ($\dot{M}CO_2$), and ammonia excretion (J_{amm}) were measured for groups of 30 pooled larvae (N = 1). Sham or AQP1a morphants were placed in glass microrespirometry chambers (internal volume of 2 ml; Loligo Systems, Tjele, Denmark). The chambers were paired with a mini-magnetic stirring system (Loligo Systems) utilizing a magnetic stir bar placed within the microrespirometry chamber but separated from the larvae by a steel mesh. The microrespirometry chambers were partially submerged in a water bath containing 28°C water. A fibre-optic O_2 electrode (FOXY AL-300; Ocean Optics, Dunedin, FL, USA) was used to monitor P_{O2} within the chamber. Prior to each experimental run, electrodes were calibrated using 'zero O_2' solution (2 g l^{-1} sodium sulphite) and air-saturated water. Water samples (50 μL) were removed from the microrespirometry chamber using gas-tight Hamilton syringes, and the total CO_2 content was measured in triplicate using a custom-built total CO_2 analyzer with the capacity to detect 6.8 μmol L^{-1} (0.3 ppm) CO_2 content. The design of the total CO_2 analyzer was based upon Cameron Instruments' Capni-Con Total CO_2 Analyzer; the instrument was designed and built by the electronics shop of the Faculty of Science at the University of Ottawa.

Each experimental run began with the placement of a group of either sham or AQP1a morphant larvae into the microrespirometry chamber. Initial water samples were removed for total CO_2 analysis, the chamber was sealed, and O_2 consumption was monitored continuously as the fall in P_{O2} over a period of 30 min. Final water samples were removed for total CO_2 content determination at 30 min. The rate of O_2 consumption was calculated from the rate of change of P_{O2} within the chamber, taking into consideration the volume of the chamber, mass of the larvae (a larval mass of 0.8 mg was used), and the solubility coefficient of O_2 in 28°C water (1.591 mmol L^{-1} mm Hg^{-1}; Boutilier *et al*, 1984). The rate of CO_2 excretion was calculated from the difference in total CO_2 content between the initial and final water samples, considering the duration of the respirometry period and the mass of the larvae. Together, these measurements allowed the calculation of the respiratory exchange ratio ($RER = \dot{M}CO_2/\dot{M}O_2$). In separate trials, the rate of ammonia excretion (J_{amm}) was calculated from measurements of ammonia concentrations in water samples (500 µL) collected at the beginning and end of a 30 min closed-chamber flux period, taking into account the mass of the larvae. Water ammonia concentrations were measured using a microplate version of the colorimetric assay of Verdouw (1978).

2.2.1.4 Determination of tissue CO_2 and ammonia concentrations in AQP1a morphants

Tissue total CO_2 concentrations of sham and AQP1a morphant larvae were assessed using the nitrilotriacetic acid (NTA) and fluoride method of Pörtner (1990). Briefly, 200 larvae (N = 1) were euthanized as described above, pooled in a 1.5 ml microcentrifuge tube, and homogenized on ice in 500 µl of 160 mM KF-6 mM Na_2NTA buffer solution using a Kimble hand-held homogenizer. To pellet cellular debris, the sample was briefly vortexed and then centrifuged at 13,000 *g* for 1 min. The resulting supernatant was removed and 1 µl of *n*-2-

octanol, an anti-foaming agent, was added. The total CO_2 content of triplicate 50 µl aliquots of the supernatant was measured using the custom-built total CO_2 analyzer.

To assess whole body ammonia concentration, 50 sham or AQP1a morphant larvae (N = 1) were collected, euthanized, flash frozen in liquid nitrogen, and stored at -80°C until analysis. Samples were homogenized, using a Kimble hand-held homogenizer, in 100 µl of 8% perchloric acid (PCA) and centrifuged at 13,000 *g* for 15 min. The supernatant was neutralized using 2 mM K_2CO_3, with the pH of each sample being brought to pH 7-8 as verified using pH paper. Supernatants were then assayed for ammonia in triplicate using a commercially available tissue ammonia assay kit (AA0100, Sigma).

2.2.2 Effect of phenylhydrazine treatment on CO_2 and ammonia excretion

To address the question of whether RBC or yolk sac epithelium AQP1a primarily is involved in CO_2 and ammonia movement, phenylhydrazine (PHZ) was used to induce haemolytic anaemia. Developing zebrafish were exposed to either 0.4 mg l^{-1} PHZ or control water from 1 to 4 dpf; the 50 ml Petri dishes containing the developing zebrafish were held in a dark 28°C incubator because PHZ is photosensitive. Water (PHZ and control) was refreshed and dead embryos were removed daily. Closed-system respirometry was carried out as described above to measure $\dot{M}O_2$, $\dot{M}CO_2$, and, in separate trials, J_{amm}. Groups of 30 PHZ-treated or control, sham or AQP1a morphant larvae (N = 1) were used for this experiment. To confirm the effectiveness of PHZ-induced anaemia, PHZ-treated and control larvae were euthanized, and fixed overnight at 4°C in 4% PFA. Subsequently, samples were washed in PBS and then stained for 10 min in the dark in a solution of *o*-dianisidine (0.6 mg ml^{-1}), 0.01 M sodium acetate (pH 4.5), 0.65% H_2O_2, and 40% (vol/vol) ethanol as described by Detrich *et al* (2005). Excess stain

was removed in a series of PBS washes (3 x 1 mL). Samples were then imaged using a model SMZ1500 microscope (Nikon Instruments, Melville, NY) to observe patterns of haeme staining.

2.2.3 Is there a functional relationship between AQP1a and Rhcg1?

2.2.3.1 Morpholino-based translational knockdown of AQP1a or Rhcg1

To study the possibility of interactions between AQP1a and Rhcg1, AQP1a expression was examined in Rhcg1 morphant larvae, and Rhcg1 expression was examined in AQP1a morphants, at both the mRNA and protein levels. Zebrafish embryos at the one- to two-cell stage were microinjected with either the AQP1a morpholino as described in section *2.2.1.1,* or with a morpholino oligonucleotide (5′-TTG GTG TTT TTG ACC ATT TTT GAT C-3′) designed to inhibit the translation of zebrafish Rhcg1 (GenBank: AB286865.1). The latter morpholino was validated by Braun *et al* (2009a), and a 4 ng embryo^{-1} dose was microinjected according to the conditions described in section *2.2.1.1.* In either case, a "sham" group of embryos was microinjected with a standard (control) morpholino (GeneTools) at the same time. Effectiveness of the AQP1a morpholino was confirmed by western blotting, tritiated water flux, and immunohistochemistry as described above. Confirmation of Rhcg1 knockdown was achieved by measuring rates of ammonia excretion in sham and Rhcg1 morphant larvae, as described above.

2.2.3.2 Analysis of AQP1a and Rhcg1 protein levels

Using a polyclonal rabbit antibody (1:1,000 dilution) developed against zebrafish Rhcg1 (see Nakada *et al,* 2007) and kindly donated by Prof. S. Hirose (Tokyo Institute of Technology), Rhcg1 protein expression was measured in sham and AQP1a morphant larvae. Similarly,

AQP1a protein abundance was also measured in sham and Rhcg1 morphant larvae. In both cases, western blotting was carried out as described in section *2.2.1.2.*

2.2.3.3 Analysis of AQP1a and Rhcg1 mRNA abundance

The mRNA abundance of AQP1a was measured in sham and Rhcg1 morphant larvae, and the mRNA abundance of Rhcg1 was measured in sham and AQP1a morphant larvae. Groups of 20 sham, AQP1a morphant, or Rhcg1 morphant larvae (N = 1) were collected, euthanized, and immediately flash-frozen in liquid nitrogen before being stored at -80°C until analysis. Using the standard TRIZOL (Invitrogen) method, total RNA was extracted from larvae. Extracted RNA was treated with DNase I (Invitrogen) according to the manufacturer's instructions, and quantified using a NanoDrop ND-1000 UV-Vis spectrophotometer. To generate cDNA, 1 μg of RNA was reverse transcribed using RevertAid M-MNuLV Reverse Transcriptase (Fermentas, Burlington, ON, Canada) and 0.2 μg μl^{-1} of random hexamer primer (IDT ReadyMade Primer) according to the manufacturer's protocol. Semi-quantitative real-time RT-PCR was carried out using a Bio Rad CFX96 real-time PCR cycler with Brilliant III SYBR Green Master Mix (Agilent Technologies, USA). The manufacturer's instructions were followed with the exception that the total volume was scaled to 10 μL instead of 25 μL. Gene-specific primers were designed using Primer3 software (http://frodo.wi.mit.edu/primer3/) and used to amplify zebrafish AQP1a.1 [forward: 5′-GCG ACT GTG GCC AGC GCT AT-3′; reverse: 5′-CGT CCC GCC GCC TTT TGT CT-3′; from Kwong *et al* (2013)] and Rhcg1 (forward: 5'-TTT GGA GGA GAG GCT GAA GA-3'; reverse: 5'-CAA AAC ACA AGG CCA CAC AC-3'); the PCR product was confirmed by direct sequencing. The ribosomal 18S subunit was used as a reference gene [forward; 5'-GGC GGC GTT ATT CCC ATG ACC-3'; reverse; 5'-GGT GGT GCC CTT CCG TCA ATT C-3'; from Kumai and Perry (2011); GenBank ID: FJ915075.1]. All

real-time RT-PCR experiments were performed using the following conditions: 95°C for 3 min, 40 cycles of 95°C for 20 s and 60°C for 20 s, with 5 min for a final extension at 72°C. For RT-PCR, cDNA samples were diluted 1:1,000 for 18S or 1:5 for AQP1a and Rhcg1. Each sample was assayed in duplicate, and no-reverse transcriptase (samples from which reverse transcriptase was omitted during cDNA synthesis) and no-template controls (samples from which RNA was omitted during cDNA synthesis) were generated and run in parallel with the samples. Standard curves were run prior to experimentation for each gene using pooled sham and morphant samples. Following the completion of 40 cycles, SYBR green dissociation curves were used to confirm the presence of single amplicons for each primer pair. All data were normalized to the expression of the housekeeping gene (18S), and expressed relative to shams, using a modification of the ΔΔCt method (Pfaffl, 2001).

2.2.4 Challenging AQP1a; high external ammonia and high pH exposures

This series of experiments was designed to examine AQP1a expression in response to two environmental challenges; high external ammonia (HEA) and high water pH. HEA is expected to impair ammonia excretion (as demonstrated by Braun *et al*, 2009b). High pH is also expected to impair ammonia excretion (Shih *et al*, 2008), but its impact on CO_2 excretion is less well studied and therefore was tested.

2.2.4.1 HEA and pH 10 water exposures; wild-type embryos

Wild-type embryos were raised from 1 to 4 dpf either in control water or in water of HEA, 500 μM NH_4Cl (Braun *et al*, 2009b). In either case, water was refreshed daily. Control and HEA larvae (20 larvae for N = 1) were euthanized as described above for protein isolation, and protein samples were probed for AQP1a using the methods described in section *2.2.1.2*.

Quantification of AQP1a protein abundance was accomplished using ImageJ. In separate trials, 20 control and HEA larvae (N = 1) were euthanized and used to isolate total RNA. Following cDNA synthesis, real-time RT-PCR analysis of AQP1a mRNA abundance was carried out according to the protocols in section *2.2.3.3*.

In a separate set of experiments, wild-type embryos were raised either in control water or in water of pH 10 from 1 to 4 dpf. As in the experiment with HEA, larvae from each group were used for protein or RNA extraction; AQP1a protein abundance was examined via western blotting and AQP1a mRNA expression via real-time RT-PCR analysis. To test the effect of exposure to pH 10 water on CO_2 excretion and ammonia excretion, groups of 4 dpf wild-type larvae (30 larvae for N = 1) were acutely exposed to pH 10 water or kept in control water and subjected to closed-system respirometry for measurement of $\dot{M}CO_2$ and $\dot{M}O_2$, or in separate trials, measurement of ammonia excretion as described in section *2.2.1.3*.

2.2.4.2 HEA and pH 10 water exposures; Rhcg1 morphants

If there are indeed interactions between Rhcg1 and AQP1a, then knockdown of Rhcg1 should increase the burden of gas transport through AQP1a. Thus, more marked fluctuations in AQP1a mRNA and protein expression in response to HEA or pH 10 exposures might be expected to occur. To test this prediction, Rhcg1 morphants were generated using the technique described in section *2.2.3.1*. The Rhcg1 morphant larvae were then subjected to HEA or pH 10 exposures followed by protein or RNA extraction, and western analysis or real-time RT-PCR, as described above for wild-type larvae.

2.2.5 Statistical analyses

Data are presented as mean values ± one standard error of the mean (SEM). SigmaPlot (version 11, Systat, Chicago, IL) was used for all statistical analyses. The level of statistical significance was set at 0.05 for all analyses. Sham and morphant larvae were compared using Student's *t*-tests for the effects of AQP1a knockdown, interactions between AQP1a and Rhcg1, and the effects of HEA or pH 10 exposures. Two-way analysis of variance (ANOVA) was used to test for effects of AQP1a knockdown or treatment with phenylhydrazine in the experiments of section *2.2.2.*

3. RESULTS

3.1 Effects of AQP1a knockdown on CO_2 and ammonia excretion

To confirm successful knockdown of AQP1a, influx of tritiated water was measured in 4 dpf larvae together with AQP1a protein abundance. A significant (Student's *t*-test, $p = 0.003$) 60% reduction in water flux was observed in AQP1a morphants (Fig. 1A). Western blot analysis revealed that AQP1a protein abundance was significantly (Student's *t*-test, $p = 0.029$) lower in AQP1a morphants relative to sham larvae; representative western blots revealed only a weak band for AQP1a at the expected size of ~27 kDa in AQP1a morphant larvae relative to that present for sham larvae (Fig. 1B). As a third, qualitative confirmation of AQP1a knockdown, immunohistochemical staining revealed AQP1a fluorescence in the RBCs of the heart and vasculature as well as in ionocytes on the yolk sac epithelium in sham larvae (Fig. 4A, B). A marked reduction in fluorescence was observed at both locations in AQP1a morphants.

Knockdown of AQP1a had no significant (Student's *t*-test, $p = 0.476$) effect on $\dot{M}O_2$ however, CO_2 excretion was significantly (Student's *t*-test, $p < 0.001$) reduced. In AQP1a morphants, $\dot{M}CO_2$ was approximately 30% lower than that of sham larvae (Fig. 2A). The calculation of respiratory exchange ratio (*RER*; $\dot{M}CO_2/\dot{M}O_2$) confirmed a specific impairment of CO_2 excretion (Student's *t*-test, $p = 0.033$) in the larvae experiencing AQP1a knockdown (Fig. 2B). This reduction in CO_2 elimination would be expected to result in CO_2 accumulation in the morphant larvae. To test this prediction, the total CO_2 contents of AQP1a morphant and sham larvae were measured. Interestingly, the expected increase in tissue CO_2 concentration was not observed in AQP1a morphant larvae; tissue CO_2 concentrations did not differ significantly (Student's *t*-test, $p = 0.233$) between morphant and sham larvae (Fig. 2C).

The effect of AQP1a knockdown on ammonia excretion was examined in parallel to the above experiments. In AQP1a morphant larvae, J_{amm} was significantly (Student's *t*-test, p = 0.018) reduced compared to sham larvae (Fig. 3A). Total ammonia content was measured for AQP1a morphant and sham larval tissues to determine whether a reduction in ammonia excretion caused ammonia to accumulate. However, tissue ammonia concentrations did not differ significantly (Student's *t*-test, p = 0.095) between the groups (Fig. 3B).

3.2 Distinguishing between possible sites of AQP1a gas transport

Figure 4 illustrates the two distinct sites of AQP1a protein expression in larval zebrafish; on the surface of RBCs and in ionocytes of the yolk sac epithelium. To assess the contribution of RBC AQP1a to CO_2 and ammonia excretion, phenylhydrazine (PHZ) was used to induce haemolytic anaemia, nominally leaving AQP1a only on the yolk sac epithelium. If RBC AQP1a contributes to CO_2 and/or ammonia excretion, then RBC elimination would be predicted to reduce CO_2 and/or ammonia excretion.

The effectiveness of PHZ-induced haemolysis was confirmed by staining larvae with the haeme-specific dye *o*-dianisidine (Fig. 5). In contrast to the lack of an effect of AQP1a knockdown on $\dot{M}O_2$ reported above, a slight but significant (two-way ANOVA, p = 0.019 for the effect of AQP1a knockdown, p = 0.371 for the effect of PHZ treatment, p = 0.655 for AQP1a knockdown x PHZ treatment) reduction in $\dot{M}O_2$ was observed in AQP1a morphants (Fig. 6A). No effect of PHZ treatment on $\dot{M}O_2$ was detected. The rate of CO_2 excretion was significantly (two-way ANOVA, $p < 0.001$ for the effect of AQP1a knockdown, p = 0.77 for the effect of PHZ treatment, p = 0.310 for AQP1a knockdown x PHZ treatment) lower (by nearly half) in AQP1a morphants compared to sham larvae, but again, PHZ treatment was without effect (Fig.

6B, C). The magnitude of the reduction in $\dot{M}CO_2$ was at least threefold greater than the decrease in $\dot{M}O_2$, resulting in significantly (two-way ANOVA, $p = 0.001$ for the effect of AQP1a knockdown, $p = 0.179$ for the effect of PHZ treatment, $p = 0.132$ for AQP1a knockdown x PHZ treatment) lower *RER* in AQP1a morphants relative to sham larvae; PHZ treatment was without effect. As well, ammonia excretion was significantly lower (two-way ANOVA, $p < 0.001$ for the effect of AQP1a knockdown, $p = 0.848$ for the effect of PHZ treatment, $p = 0.310$ for AQP1a knockdown x PHZ treatment) in AQP1a morphants compared to sham larvae but no effect of PHZ treatment was detected (Fig. 7).

3.3 Interactions between AQP1a and Rhcg1

The potential for interactions between AQP1a and Rhcg1 was examined by measuring, in a series of mirrored experiments, AQP1a expression in Rhcg1 morphant larvae, and Rhcg1 expression in AQP1a morphants, at both the mRNA and protein levels. Neither AQP1a mRNA nor protein abundance was significantly (Student's *t*-tests, $p = 0.310$ for mRNA abundance and $p = 0.413$ for protein concentration) increased in Rhcg1 morphants compared to sham larvae (Fig. 8A, B). Similarly, no significant (Student's *t*-tests, $p = 0.659$ for mRNA abundance and $p = 0.499$ for protein concentration) differences in Rhcg1 protein or mRNA abundance were observed in AQP1a morphants relative to sham larvae (Fig. 8C, D).

3.4 Effect of high external ammonia (HEA) and pH 10 exposures on AQP1a expression

Exposure of wild-type zebrafish larvae to 500 μM NH_4Cl (HEA) for three days produced no significant differences in AQP1a expression compared to control conditions, as demonstrated by both real-time PCR (Fig. 10A; Student's *t*-test, $p = 0.64$) and western blot analysis (Fig. 10B; Student's *t*-test, $p = 0.498$). Although no significant difference in AQP1a mRNA expression was

detected following a 3-day exposure to pH 10 water (Fig. 10C; Student's *t*-test, $p = 0.137$), this exposure triggered a marked decrease in AQP1a protein expression, lowering AQP1a protein levels almost to the limit of detection of the western blot analysis (Fig. 10D; Student's *t*-test, $p < 0.001$). Exposure to pH 10 did not result in significant differences in *RER* between pH 10-exposed and control (normal water pH) larvae (Fig. 9B; Student's *t*-test, $p = 0.728$); $\dot{M}CO_2$ was slightly but not significantly reduced in the pH 10-exposed fish and when corrected for variations in $\dot{M}O_2$, the trend disappeared (Fig. 9A; Student's *t*-test, $p = 0.310$ for $\dot{M}CO_2$ and $p = 0.145$ for $\dot{M}O_2$). However, J_{amm} was significantly lower following acute exposure to pH 10 water than under control conditions (Fig. 9C; Student's *t*-test, $p = 0.045$).

The exposures to HEA and alkaline water were repeated in Rhcg1 morphant larvae, to test the prediction that knockdown of one of the two (known) multi-functional gas channels would increase the burden of CO_2 and ammonia transport *via* AQP1a. Thus, more pronounced variations in AQP1a expression in response to these exposures were predicted to occur. Knockdown of Rhcg1 was confirmed by measuring ammonia flux; J_{amm} decreased significantly in Rhcg1 morphants compared to shams (3.38 ± 0.73 *versus* 5.87 ± 0.45 μmol L^{-1} under control conditions; Student's *t*-test, $p = 0.027$). Although AQP1a mRNA abundance tended to increase following exposure of Rhcg1 morphant larvae to either HEA or pH 10 water, the differences were not statistically significant in either situation (Fig. 11A, C; Student's *t*-test, $p = 0.075$ for HEA and $p = 0.116$ for pH 10 water). Exposure of Rhcg1 morphants to HEA did provoke a significant increase in AQP1a protein abundance compared to control conditions (Fig. 11C; Student's *t*-test, $p = 0.049$). With the removal of one data point in the HEA-exposed group that appeared to be a statistical outlier (Grubbs' test), the statistical significance of the difference increased (Student's *t*-test, $p = 0.002$). As in the wild-type larvae, exposure of Rhcg1 morphants

to pH 10 water triggered a significant decrease in AQP1a protein expression (Fig. 11D; Student's *t*-test, $p = 0.009$).

Figure 1. Confirmation of AQP1a knockdown in zebrafish, *Danio rerio,* larvae by tritiated water flux and western blot analysis. A) Tritiated water flux of 4 dpf AQP1a morphants (AQP1a-MO) was significantly lower than that of sham-injected larvae (Student's *t*-test, $p = 0.003$, N = 6). B) The protein abundance of AQP1a was significantly reduced in 4 dpf AQP1a morphants relative to sham larvae (Students *t* test, $p = 0.029$, N = 4). The inset panel presents a representative western blot demonstrating a single immunoreactive band for AQP1a at the expected size of 27 kDa; this band was reduced in intensity (relative to the control, ß-actin) in AQP1a morphant larvae. Data are mean values + SEM and an asterisk indicates a significant difference between sham and AQP1a morphant larvae.

(A)

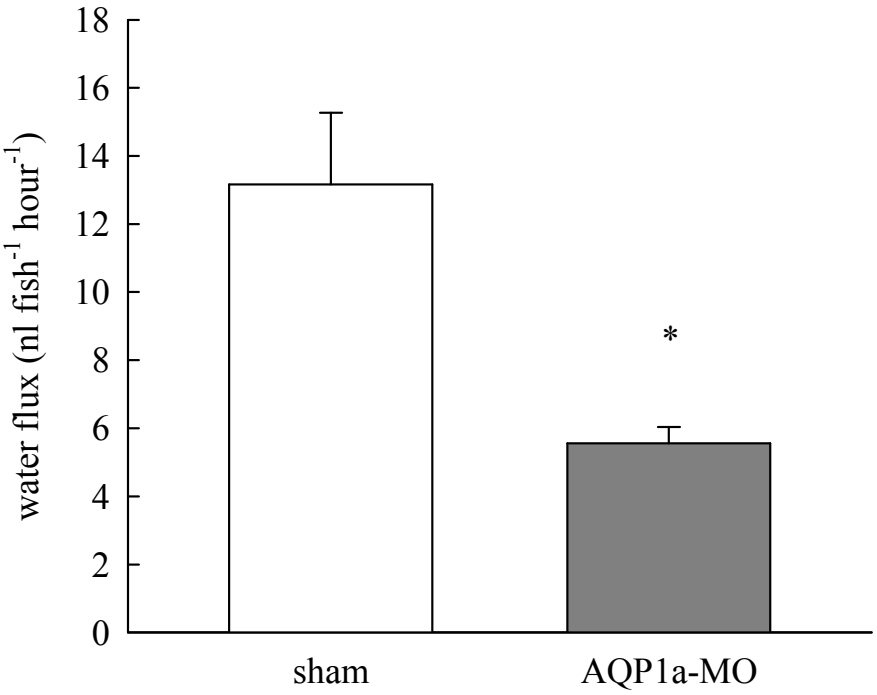
18
16
14
12
10
8
6
4
2
0
water flux (nl fish-1 hour-1)
*
sham
AQP1a-MO

(B)

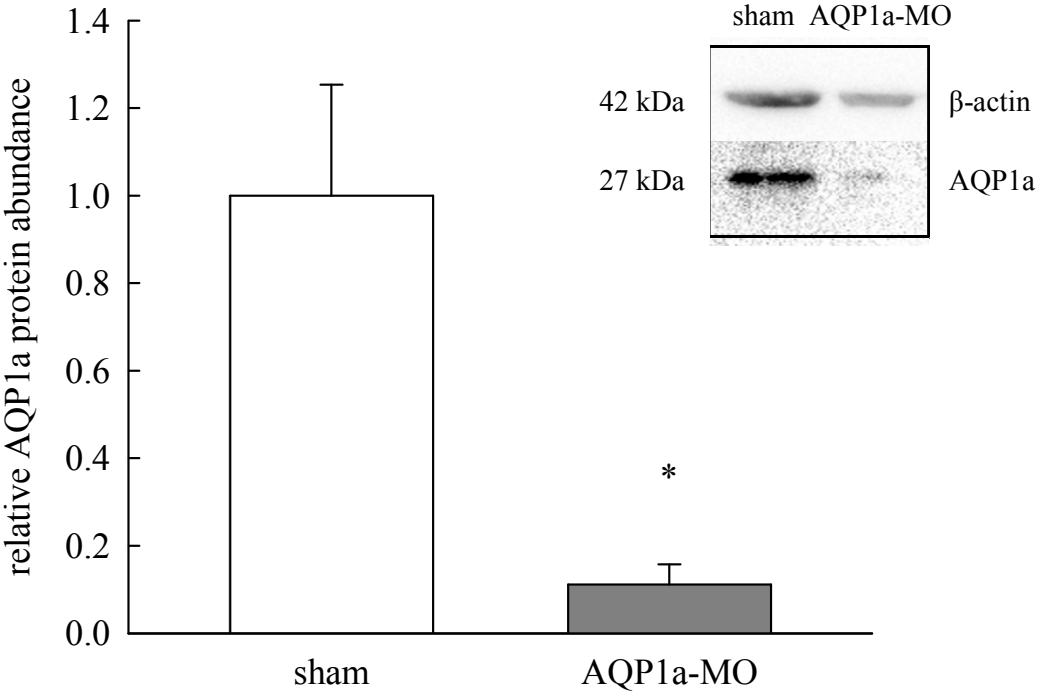
1.4
1.2
1.0
0.8
0.6
0.4
0.2
0.0
relative AQP1a protein abundance
*
sham
AQP1a-MO
sham AQP1a-MO
42 kDa
β-actin
27 kDa
AQP1a

Figure 2. Effect of AQP1a knockdown on A) the rates of O_2 uptake ($\dot{M}O_2$) and CO_2 excretion ($\dot{M}CO_2$), B) the respiratory exchange ratio (*RER*), and C) tissue total CO_2 concentrations in 4 dpf zebrafish (*Danio rerio*) larvae. Values are means + SEM. Significant differences between sham and AQP1a morphant larvae (AQP1a-MO) are indicated by asterisks. In panel A, $\dot{M}CO_2$, but not $\dot{M}O_2$, was significantly reduced in AQP1a morphants compared to sham-injected larvae (N = 7; Student's *t*-test, $p = 0.476$ for $\dot{M}O_2$, < 0.001 for $\dot{M}CO_2$). Similarly, *RER* (panel B) also was significantly lowered following knockdown of AQP1a (N = 7; Student's *t*-test, $p = 0.033$). However, tissue total CO_2 content was not significantly different following AQP1a knockdown (panel C, N = 5; Student's *t*-test, $p = 0.233$).

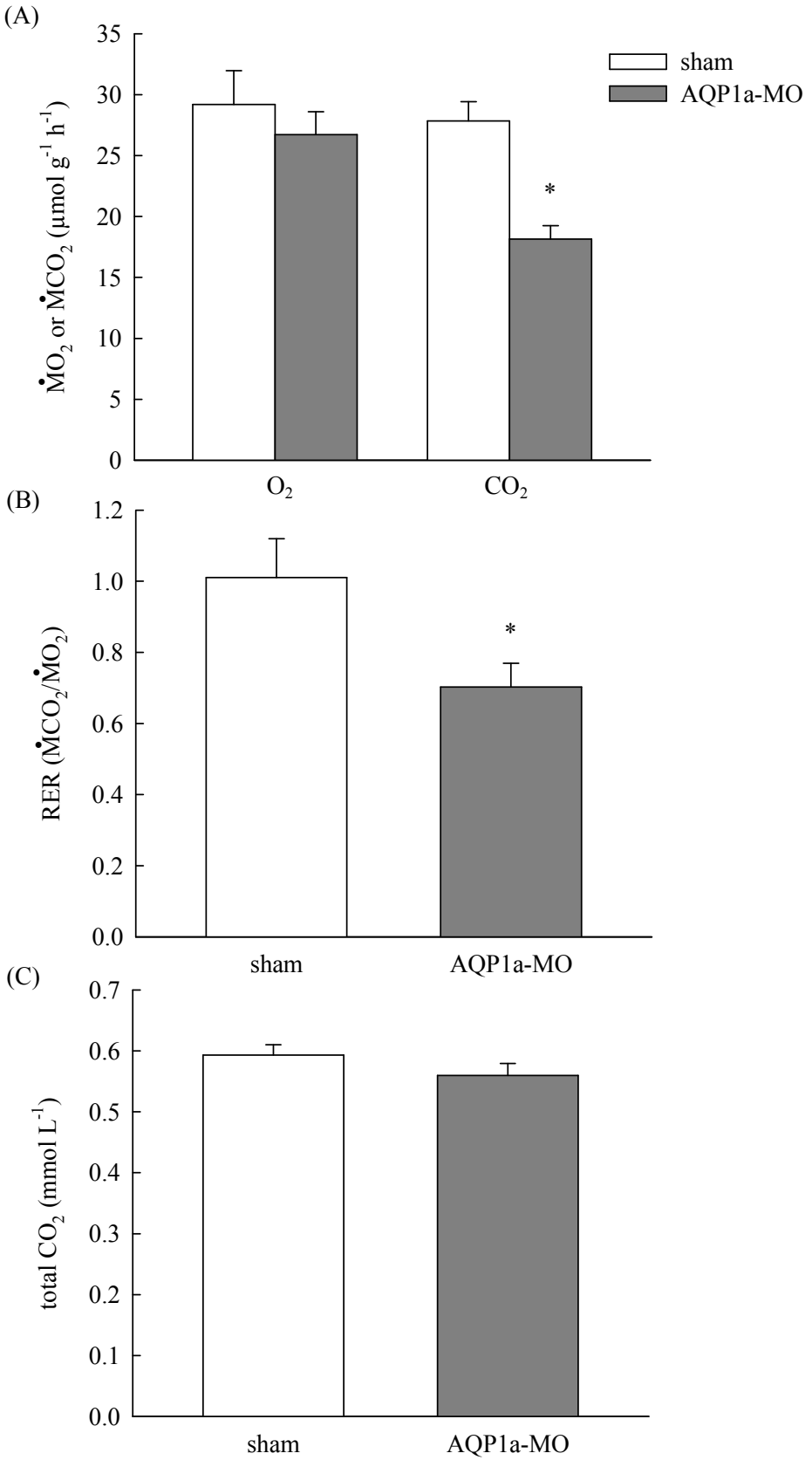
(A)
sham
AQP1a-MO
$\dot{M}O_2$ or $\dot{M}CO_2$ (μmol g^{-1} h^{-1})
35
30
25
20
15
10
5
0
*
O_2
CO_2
(B)
RER ($\dot{M}CO_2/\dot{M}O_2$)
1.2
1.0
0.8
0.6
0.4
0.2
0.0
*
sham
AQP1a-MO
(C)
total CO_2 (mmol L^{-1})
0.7
0.6
0.5
0.4
0.3
0.2
0.1
0.0
sham
AQP1a-MO

Figure 3. Effect of AQP1a knockdown on A) ammonia excretion (J_{amm}) and B) tissue ammonia concentration ([ammonia]) in 4 dpf zebrafish (*Danio rerio*) larvae. Values are means + 1 SEM and significant differences between AQP1a morphants (AQP1a-MO) and sham larvae are indicated by asterisks. Panel A demonstrates that ammonia excretion was significantly reduced in AQP1a morphants compared to sham larvae (N = 12-13; Student's *t*-test $p = 0.018$). However, total ammonia content was not significantly different following AQP1a knockdown (panel B, N = 5; Student's *t*-test, $p = 0.095$).

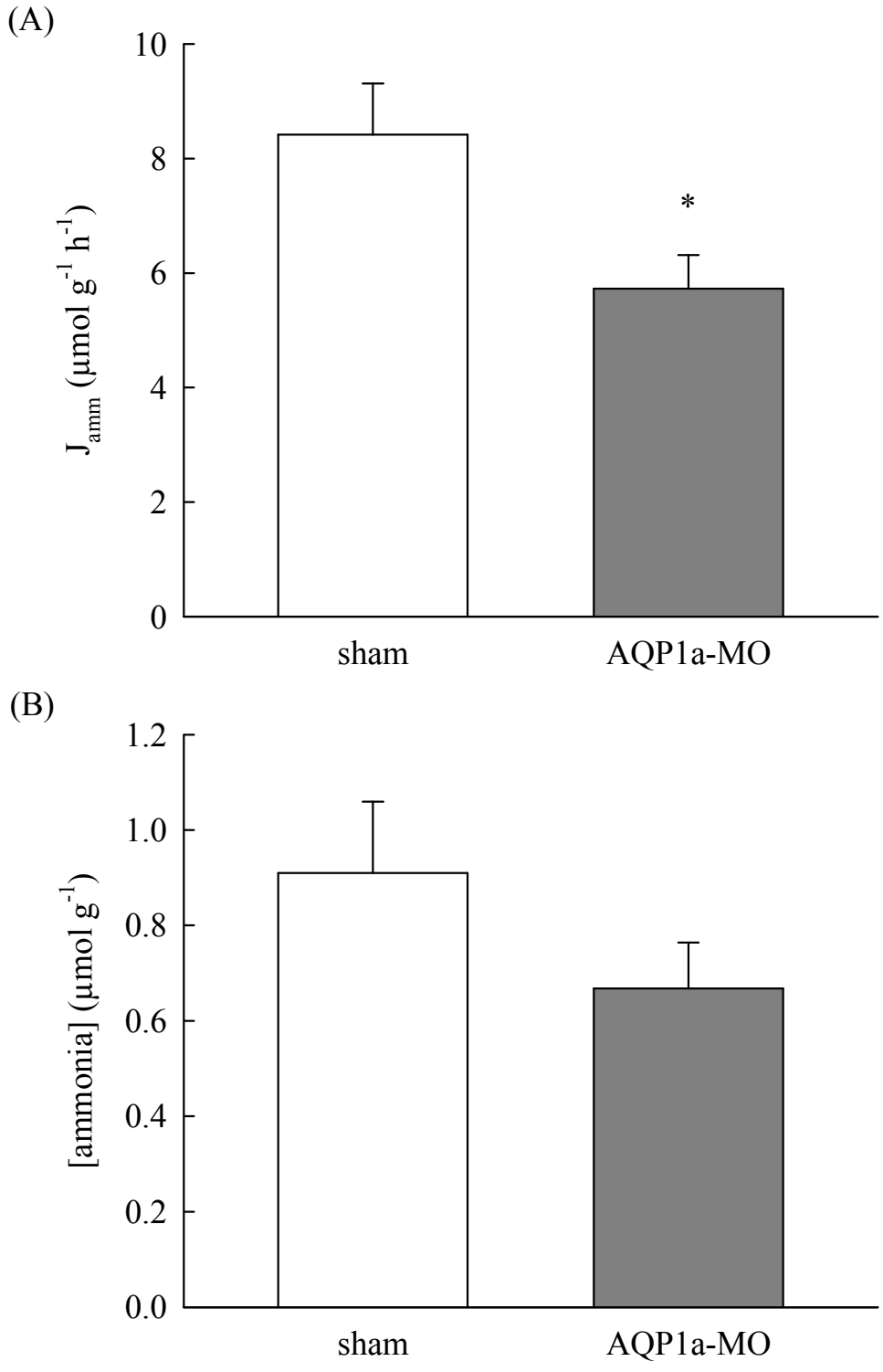
(A)
10
8
6
4
2
0
J_{amm} (μmol g^{-1} h^{-1})
*
sham
AQP1a-MO
(B)
1.2
1.0
0.8
0.6
0.4
0.2
0.0
[ammonia] (μmol g^{-1})
sham
AQP1a-MO

Figure 4. Fluorescent immunohistochemistry of AQP1a in 4 dpf zebrafish (*Danio rerio*) larvae. Panels A and B are representative confocal micrographs of AQP1a immunofluorescence in sham (A) and AQP1a-morphant (B) larvae. In the sham larva, AQP1a staining (arrows) is associated with RBCs in the heart, gill, and fin vasculature; fluorescence in these areas is eliminated following AQP1a knockdown. Scale bar = 200 μm. Images provided courtesy of Dr. Yusuke Kumai (unpublished data). Panels C and D are representative, higher magnification images of AQP1a fluorescence in individual RBCs of the gill vasculature (C; scale bar = 25 μm) and in the ionocytes of the yolk sac epithelium (D; scale bar = 100 μm) in sham larvae. Images provided courtesy of Dr. Raymond Kwong (unpublished data).

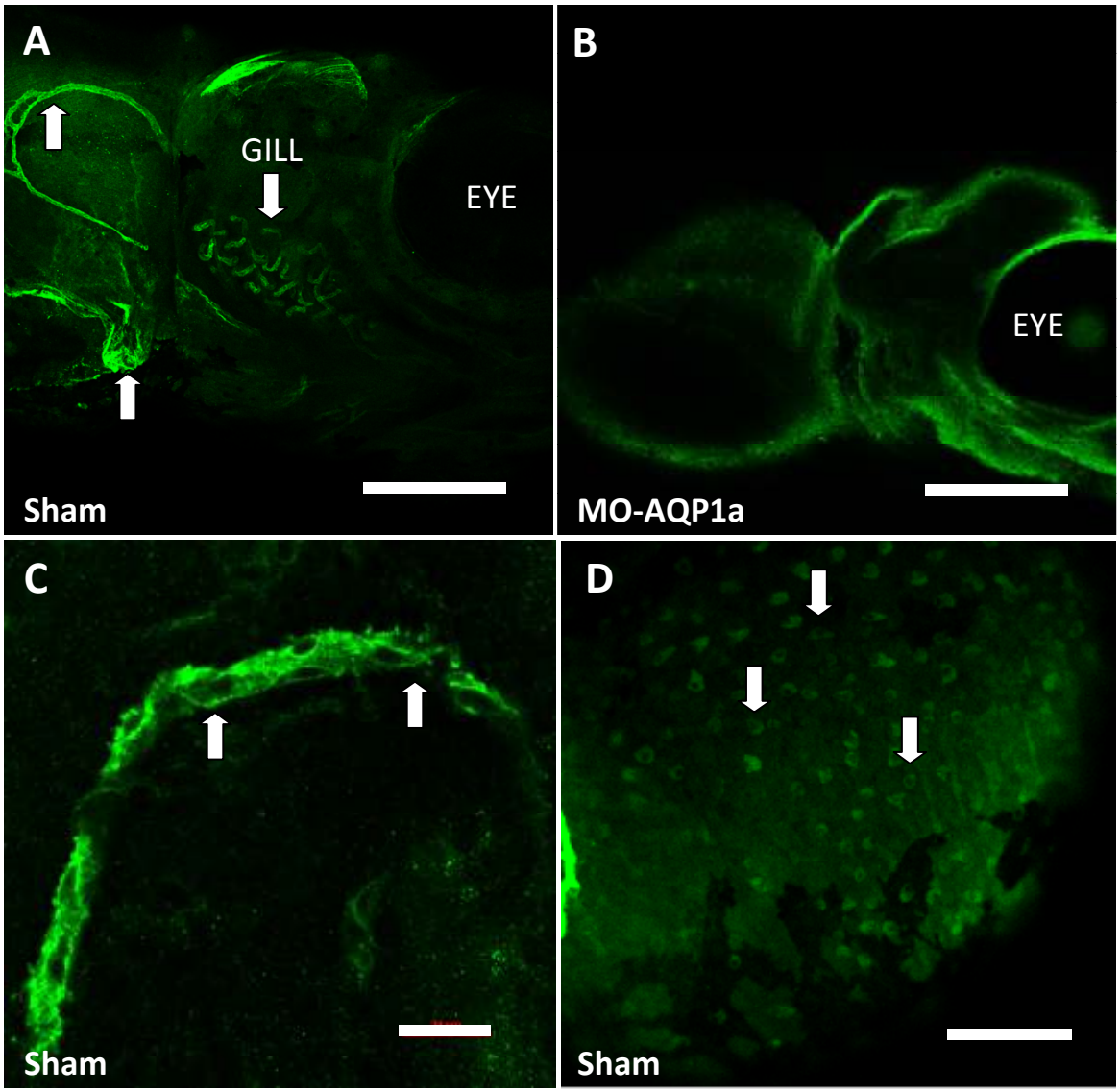
A
GILL
EYE
Sham
B
EYE
MO-AQP1a
C
Sham
D
Sham

Figure 5. Phenylhydrazine (PHZ; 0.4 mg L^{-1}) treatment reduced staining of RBC-associated haemes in 4 dpf zebrafish (*Danio rerio*) larvae. Larvae were stained with o-dianisidine, a haeme-specific dye that therefore functions as a RBC marker (arrows in panel A). Absence of haeme staining in the heart and vasculature (panel B) was indicative of PHZ-related haemolysis.

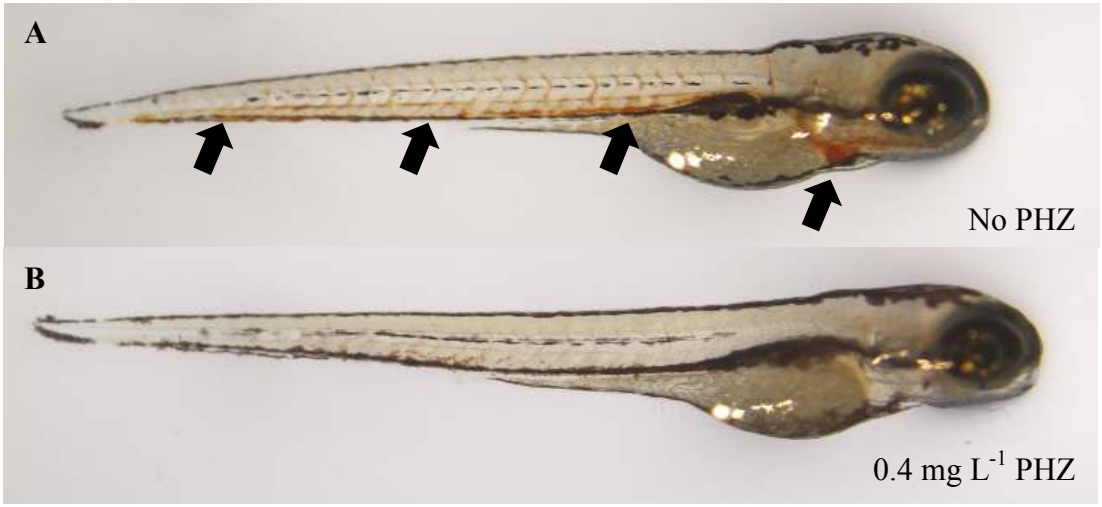
A
No PHZ
B
0.4 mg L-1 PHZ

Figure 6. Effects of phenylhydrazine (PHZ; indicated by hatched bars) treatment on A) the rate of O_2 uptake ($\dot{M}O_2$), B) the rate of CO_2 excretion ($\dot{M}CO_2$), and C) the respiratory exchange ratio (*RER*) in 4 dpf zebrafish (*Danio rerio*) sham-injected or AQP1a morphant (AQP1a-MO) larvae. Values are means + 1 SEM, and groups that share a letter are not significantly different from each other. Panel A demonstrates that $\dot{M}O_2$ was significantly reduced in AQP1a morphant larvae (grey bars) compared to shams (white bars) (N = 5; two-way ANOVA, see text for statistical details), with no significant effect of PHZ treatment. Similarly, $\dot{M}CO_2$ was decreased in AQP1a morphants relative to sham larvae with no significant effect of PHZ treatment (panel B, N = 5; two-way ANOVA, see text for statistical details). In panel C, treatment with PHZ did not significantly lower *RER*, but *RER* was significantly reduced in AQP1a morphants compared to sham larvae (N = 5; two-way ANOVA, see text for statistical details).

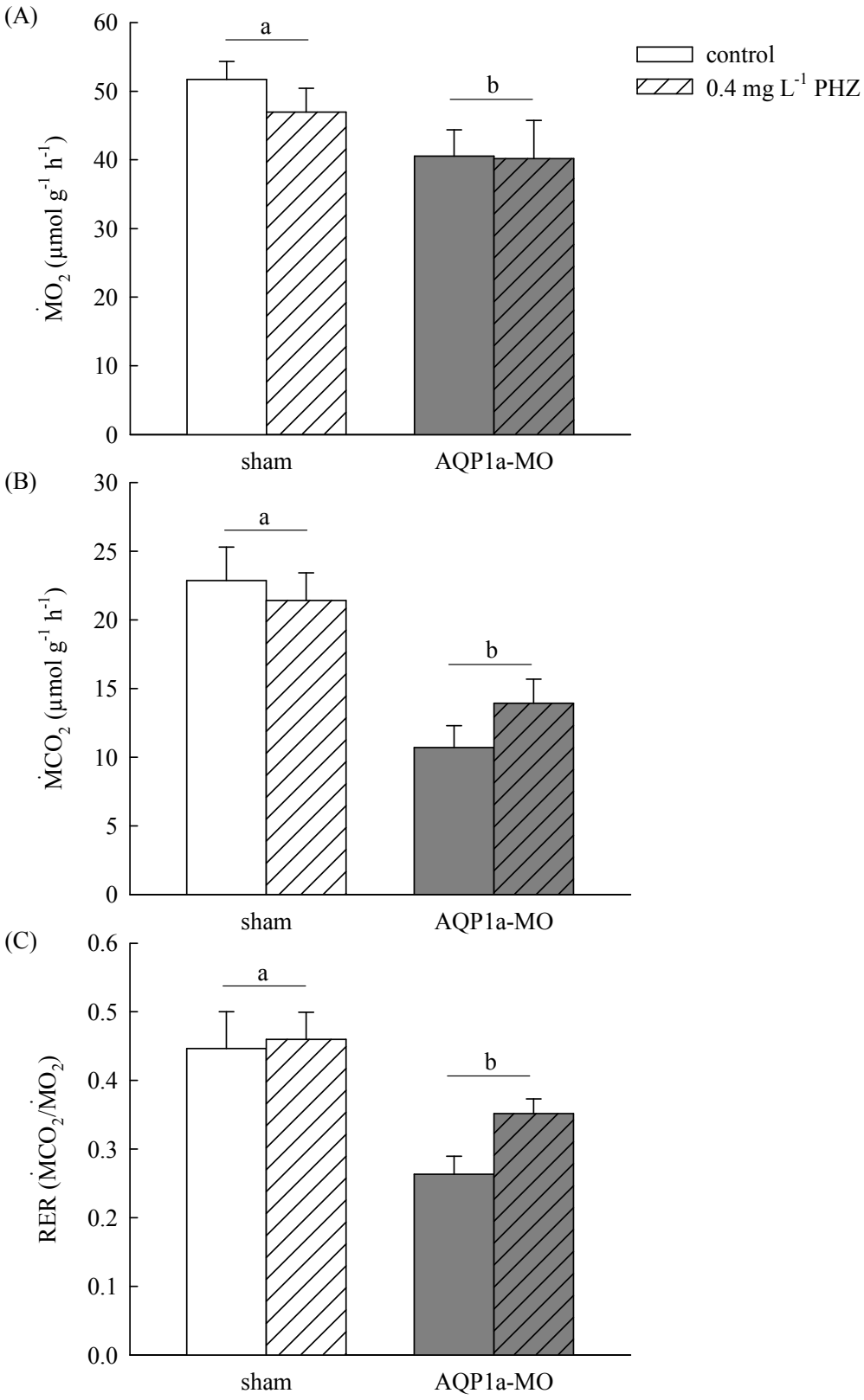
(A)
60
50
40
30
20
10
0
$\dot{M}O_2$ (μmol g^{-1} h^{-1})
a
b
control
0.4 mg L^{-1} PHZ
sham
AQP1a-MO
(B)
30
25
20
15
10
5
0
$\dot{M}CO_2$ (μmol g^{-1} h^{-1})
a
b
sham
AQP1a-MO
(C)
0.6
0.5
0.4
0.3
0.2
0.1
0.0
RER ($\dot{M}CO_2$/$\dot{M}O_2$)
a
b
sham
AQP1a-MO

Figure 7. Effects of phenylhydrazine (PHZ; indicated by hatched bars) treatment on ammonia excretion (J_{amm}) in AQP1a morphant (AQP1a-MO; grey bars) and sham (white bars) 4 dpf zebrafish (*Danio rerio*) larvae. Data are presented as means + SEM and groups that share a letter are not significantly different from each other. Treatment with PHZ did not significantly affect ammonia excretion, but J_{amm} was reduced in AQP1a morphants relative to sham larvae (N = 5-6; two-way ANOVA, see text for statistical details).

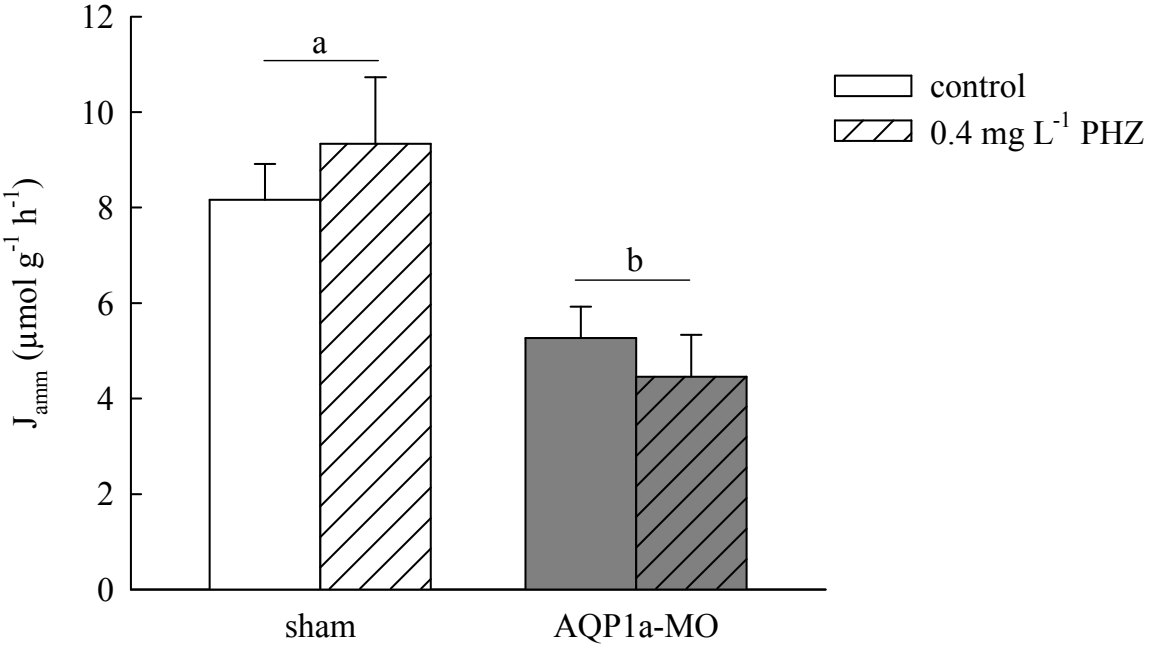
12
10
8
6
4
2
0
J_{amm} (μmol g^{-1} h^{-1})
a
b
control
0.4 mg L^{-1} PHZ
sham
AQP1a-MO

Figure 8. Relationships between AQP1a and Rhcg1 mRNA and protein abundance in 4 dpf zebrafish (*Danio rerio*) larvae experiencing AQP1a (AQP1a-MO) or Rhcg1 (Rhcg1-MO) knockdown. Values are means + SEM and no significant differences between groups were detected (Student's *t*-tests, $p = 0.659$, 0.499, 0.310 and 0.413 for panels A to D, respectively). Panels A and B present Rhcg1 mRNA (A) and protein levels (B) in AQP1a morphants relative to shams (N = 6-7). Panels C and D present AQP1a mRNA (C) and protein (D) abundance in Rhcg1 morphants relative to shams (N = 4-6). Representative western blots are included in each of panels B and D. Normalization of mRNA abundance was relative to 18S, whereas protein levels were normalized to ß-actin.

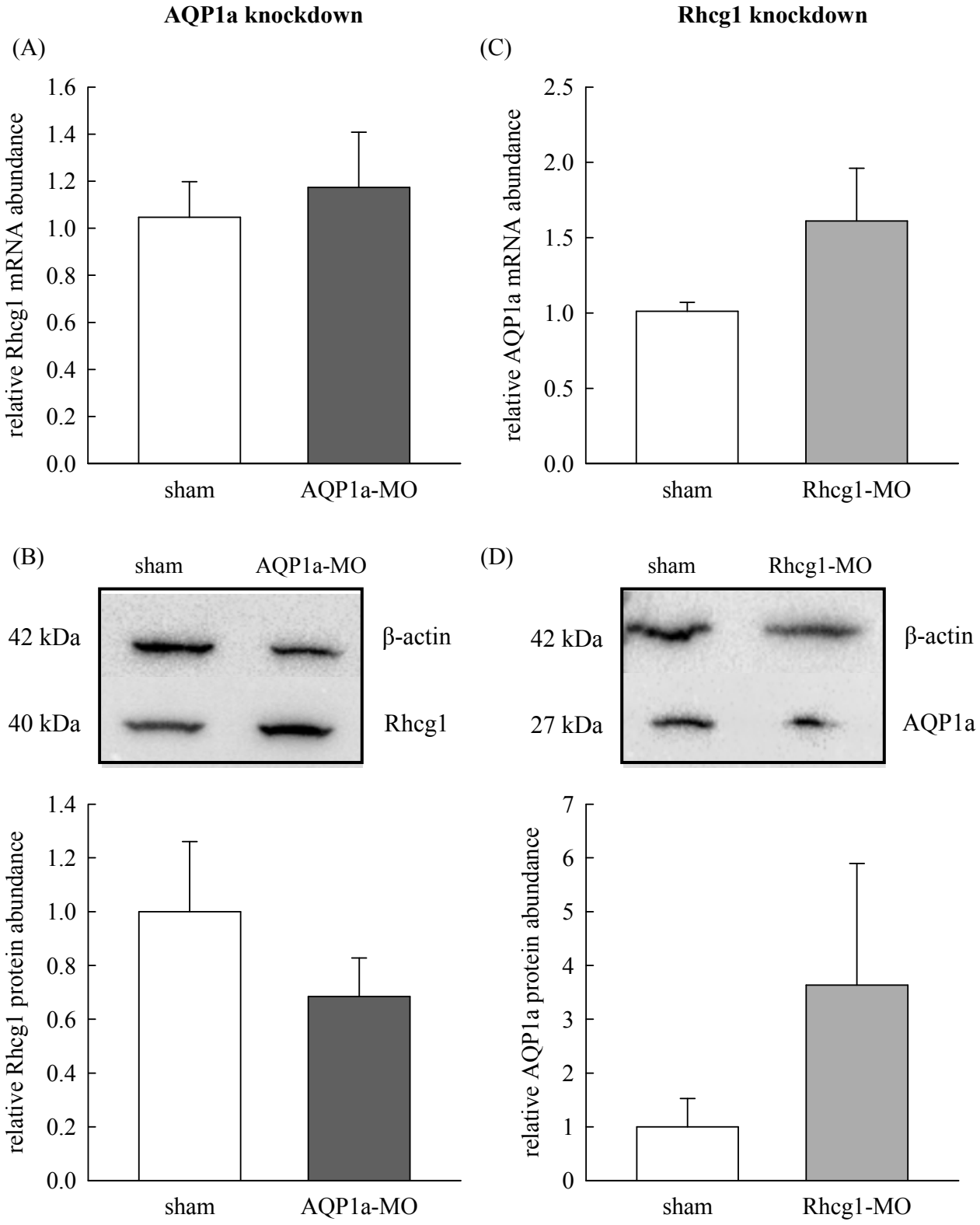
AQP1a knockdown
Rhcg1 knockdown
(A)
(C)
relative Rhcg1 mRNA abundance
relative AQP1a mRNA abundance
sham
AQP1a-MO
Rhcg1-MO
(B)
(D)
42 kDa
40 kDa
27 kDa
β-actin
Rhcg1
AQP1a
relative Rhcg1 protein abundance
relative AQP1a protein abundance

Figure 9. Effect of acute exposure to pH 10 water on A) the rates of O_2 uptake ($\dot{M}O_2$) and CO_2 excretion ($\dot{M}CO_2$), B) the respiratory exchange ratio (*RER*), and C) ammonia excretion (J_{amm}) in 4 dpf wild-type zebrafish (*Danio rerio*) larvae. Values are means + 1 SEM. An asterisk indicates a significant difference from the corresponding control value. In Panel A, both $\dot{M}CO_2$ and $\dot{M}O_2$ were unaffected following acute exposure to pH 10 water (N = 6; Student's *t*-test, $p = 0.310$ for $\dot{M}CO_2$, 0.145 for $\dot{M}O_2$). Panel B demonstrates that *RER* was not significantly different between larvae acutely exposed to pH 10 water and those exposed to control conditions (N = 6; Student's *t*-test $p = 0.728$). However, ammonia excretion was significantly reduced by acute pH 10 exposure (Panel C, N = 8; Student's *t* test $p = 0.045$).

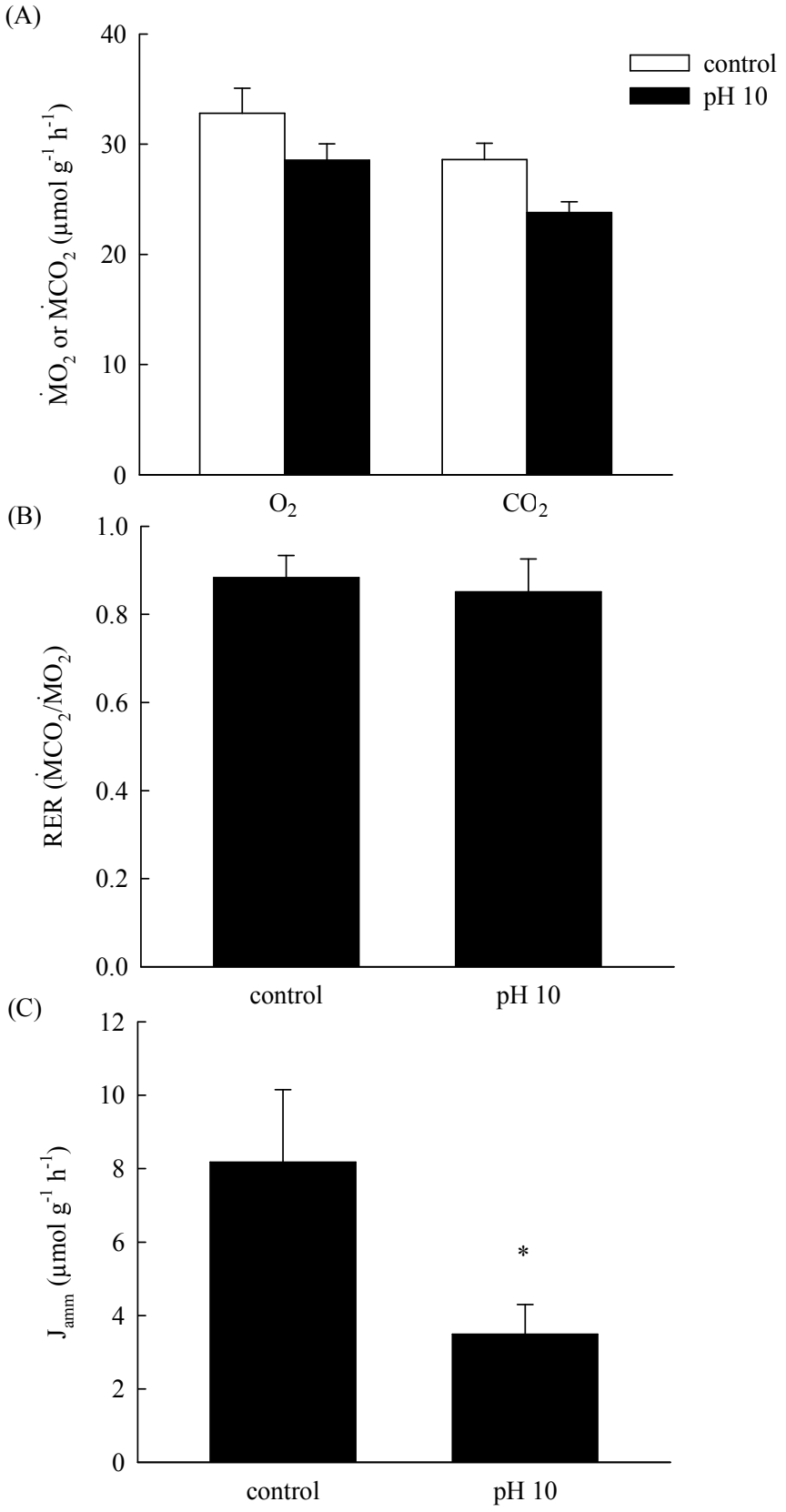
(A)
40
30
20
10
0
control
pH 10
$\dot{M}O_2$ or $\dot{M}CO_2$ (µmol g^{-1} h^{-1})
O_2
CO_2
(B)
1.0
0.8
0.6
0.4
0.2
0.0
RER ($\dot{M}CO_2/\dot{M}O_2$)
control
pH 10
(C)
12
10
8
6
4
2
0
J_{amm} (µmol g^{-1} h^{-1})
*
control
pH 10

Figure 10. Effect of high external ammonia (HEA) or pH 10 water exposure on AQP1a mRNA and protein expression in 4 dpf wild-type zebrafish (*Danio rerio*) larvae. Panels A and B present AQP1a mRNA (A) and protein (B) levels in larvae following 72-h exposure to 500 μM NH_4Cl (N = 7-8; Student's *t*-test $p = 0.64$ for A, 0.498 for B). Panels C and D present AQP1a mRNA (C) and protein (D) levels following 72-h exposure to pH 10 water (N = 7-8; Student's *t*-test $p = 0.137$ for panel C, $p < 0.001$ for panel D). Values are means + 1 SEM; mRNA values were expressed relative to 18S mRNA expression levels whereas protein levels were normalized to ß-actin. An asterisk indicates a significant difference between control and treated zebrafish larvae. Representative western blots are included in panels B and D.

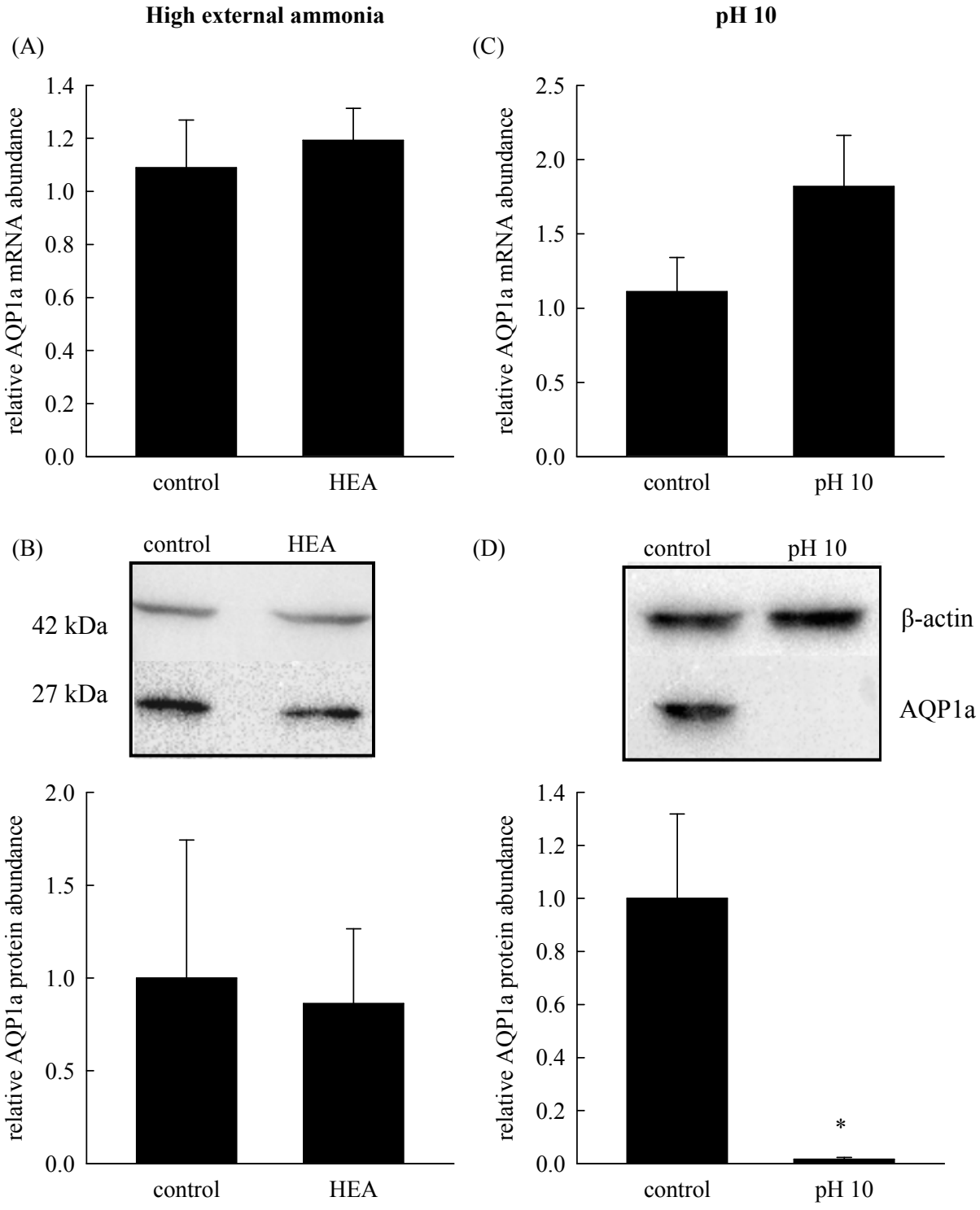
High external ammonia
pH 10
(A)
(C)
relative AQP1a mRNA abundance
1.4
1.2
1.0
0.8
0.6
0.4
0.2
0.0
control
HEA
2.5
2.0
1.5
1.0
0.5
0.0
control
pH 10
(B)
(D)
control
HEA
control
pH 10
42 kDa
27 kDa
β-actin
AQP1a
relative AQP1a protein abundance
2.0
1.5
1.0
0.5
0.0
1.4
1.2
1.0
0.8
0.6
0.4
0.2
0.0
*

Figure 11. Effect of high external ammonia (HEA) or pH 10 water exposure on AQP1a mRNA and protein expression in 4 dpf Rhcg1 morphant zebrafish (*Danio rerio*) larvae. Values are means + 1 SEM and significant differences between treatment groups are indicated by asterisks. Panels A and B present AQP1a mRNA (A) and protein (B) levels in Rhcg1 morphant larvae following 72-h exposure to 500 μM NH_4Cl (N = 5-6; Student's *t*-test $p = 0.075$ for panel A and 0.009 for panel B). Panels C and D present AQP1a mRNA (C) and protein (D) levels in Rhcg1 morphant larvae 72-h exposure to pH 10 water (N = 5-6; Student's *t*-test, $p = 0.116$ for panel C and $p = 0.009$ for panel D). The expression of mRNA levels was relative to 18S mRNA expression levels, whereas protein levels were normalized to ß-actin. Representative western blots are included in panels B and D.

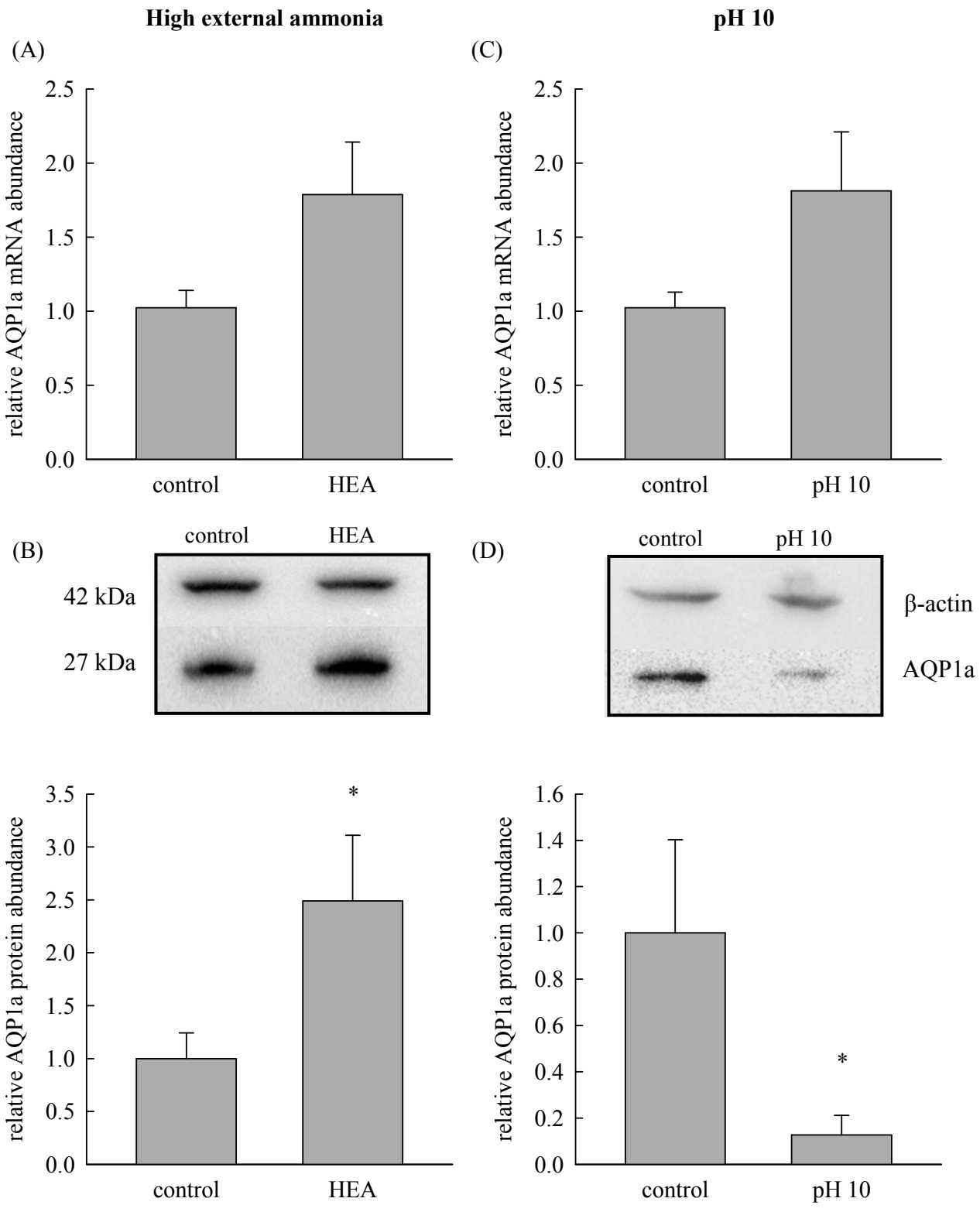
High external ammonia
pH 10
(A)
(C)
relative AQP1a mRNA abundance
2.5
2.0
1.5
1.0
0.5
0.0
control
HEA
pH 10
(B)
(D)
control
HEA
pH 10
42 kDa
27 kDa
β-actin
AQP1a
relative AQP1a protein abundance
3.5
3.0
2.5
2.0
1.5
1.0
0.5
0.0
1.6
1.4
1.2
1.0
0.8
0.6
0.4
0.2
*

4. DISCUSSION

The results of the present study suggest a physiologically-significant role for AQPs outside of their traditional osmoregulatory function. Specifically, the data demonstrate that AQP1a is involved in CO_2 and ammonia excretion in larval zebrafish, and thus provide significant new information to our understanding of gas transfer in developing teleost fish. Further, they support current ideas about gas transfer during early development not relying on circulating RBCs. Because the Rh glycoproteins were previously identified as multi-functional gas channels involved in ammonia and CO_2 movement (Perry *et al*, 2010), the present study explored a potential relationship between AQP1a and Rhcg1. In the following discussion I will make a case for AQPs as a second class of multi-functional gas channel.

4.1 Experimental approaches

The availability of microinjection techniques and morpholino oligonucleotide technology were key factors in the choice of zebrafish as the study organism. Additionally, there is a large body of literature available for this species, including the previous *in vitro* work on CO_2 and ammonia movement using zebrafish AQP1a (Chen *et al*, 2010) and the translational knockdown study of Rhcg1 and its impact on CO_2 excretion in zebrafish larvae (Perry *et al*, 2010). Morpholino antisense oligonucleotides have been the preferred method of gene knockdown in recent years owing to their stability, low toxicity, and specificity. Occasionally, use of translation-blocking morpholinos can produce off-target effects, such as cell death, gross morphological abnormalities, or developmental delay (Bill *et al*, 2009). However, with dosage control and careful screening, these effects can be essentially eliminated. As an alternative to morpholino-based knockdown, the use of an AQP inhibitor such as $HgCl_2$ was briefly considered

for the present study (Carlsson *et al*, 1996; Liakopoulos *et al*, 2006; Yukutake *et al*, 2008). However, $HgCl_2$ is a broad inhibitor of all AQPs (therefore not specific to AQP1a) and pilot studies in larval zebrafish demonstrated significant mortality following application of $HgCl_2$.

A translation-blocking morpholino was designed against zebrafish AQP1a and the effect of the knockdown on CO_2 and ammonia excretion across the larval body surface was assessed. In the present study, successful knockdown of the AQP1a protein was demonstrated by a 50-80% reduction in protein levels at 4 dpf concurrent with an inhibition of water influx. In another series of experiments, a similar morpholino approach was used to knock down Rhcg1, and successful knockdown was confirmed *via* measurement of ammonia flux (Braun *et al*, 2009a). A 50% reduction of *Jamm* was typical following Rhcg1 knockdown. The choice of 4 dpf larvae for the current study reflected a variety of factors. First, zebrafish larvae do not require gills for gas exchange until 14 dpf, and thus all gas transfer would be expected to occur across the skin prior to this time (Rombough, 2002). As well, CO_2 and ammonia excretion both increase post-hatch (Gilmour *et al*, 2009; Braun *et al*, 2009a), reaching more readily-detectable levels by 4 dpf.

4.2 AQP1a knockdown reduced CO_2 excretion

Using the *in vitro* expression of zebrafish AQP1a in *Xenopus* oocytes, AQP1a was found to be capable of conducting CO_2 (Chen *et al*, 2010). However, the physiological relevance of AQP1a in terms of CO_2 movement in living organisms has been studied only rarely. For example, AQP1 was implicated as a major pathway for CO_2 uptake during photosynthesis in the tobacco plant (Uehlein *et al*, 2003). As well, AQP1 plays a major role in bicarbonate reabsorption in the proximal tubule of the nephron (Boron, 2006); the first critical step of this process is the apical entry of CO_2 and acidification of the cell. Finally, AQP1 is understood to be

a major pathway for CO_2 flux across the human RBC plasma membrane (Endeward *et al*, 2006). The findings of the present study demonstrate for the first time in teleosts that AQP1 contributes to CO_2 excretion. Translational knockdown of AQP1a in zebrafish larvae produced a significant and specific reduction in whole body CO_2 excretion ($\dot{M}CO_2$) in the absence of any effect on O_2 uptake, in accordance with the findings of Chen *et al* (2010). While $\dot{M}O_2$ values in the present study were comparable to those reported in Gilmour *et al* (2009), $\dot{M}CO_2$ and *RER* values reported here were somewhat lower [25-30 μmol g^{-1} h^{-1} *versus* ~50 μol g^{-1} h^{-1} in Gilmour *et al* (2009)]. The reasons for these differences are not obvious, but one possibility is an injection effect – the data in Gilmour *et al* (2009) reflected 4 dpf wild-type larvae instead of the sham-injected larvae used in the present study.

An increase in tissue total CO_2 content of AQP1a morphant larvae as a consequence of the reduction in CO_2 elimination would be predicted to occur together with a concomitant lowering of tissue pH (respiratory acidosis); the latter might be corrected through HCO_3^- accumulation (Perry *et al*, 2003; Perry and Gilmour, 2006). Using a protocol modified from Pörtner *et al* (1990), larval tissue was homogenized in a pH-stable buffer containing metabolic inhibitors, and total CO_2 content was measured using a custom-built total CO_2 analyzer. The absence of a difference in total CO_2 content between sham and AQP1a morphant larvae was unexpected, but could have been a consequence of technical issues experienced with the experimental apparatus during these measurements. Sample injection resulted in foaming that was only minimally resolved by co-injection of the anti-foaming reagent *n*-2-octanol; it is likely that this problem affected the reliability of the tissue total CO_2 content data. Furthermore, it is possible that significant CO_2 was lost during homogenization owing to the pH of the homogenization buffer; use of a more alkaline buffer could help to trap CO_2 in solution.

The pathway through which CO_2 traverses AQP1a remains unclear. Aquaporins assemble in the plasma membrane as tetramers, with each monomer acting as an independent water channel and a larger pore forming at the centre of the tetrameric arrangement (Verbavatz *et al*, 1993; Wang *et al,* 2007). As a linear molecule with a diameter similar to that of water, CO_2 should be capable of passing through the AQP1a monomers (Wang *et al*, 2007). However, a number of different computer simulations have calculated the energetics associated with CO_2 permeability *via* AQP1, and some have suggested that the large "fifth" central pore would be a more energetically-favourable route through which CO_2 (and potentially other gases) might pass (Wang *et al*, 2007). Presently, computational bioinformatics methods provide the only means of investigating this issue; there are no experimental protocols for directly tracking the pathway that gases might travel through AQP1a.

4.3 AQP1a knockdown reduced ammonia excretion

Whole-body ammonia excretion (J_{amm}) was significantly reduced, by approximately one-third, in AQP1a morphant larvae, indicating a role for AQP1a in nitrogenous waste elimination in larval zebrafish. This finding was in accordance with previous *in vitro* work by Chen *et al* (2010) that demonstrated that zebrafish AQP1a was permeable to ammonia. In the present study, J_{amm} values for sham-injected larvae were similar to those reported previously (Braun *et al*, 2009a; Perry *et al*, 2010; Shih *et al*, 2008), as were tissue ammonia concentrations (Braun *et al* 2009a). Prior to hatching, nitrogen excretion in developing zebrafish is dominated by urea excretion, but by 4 dpf, ammonia excretion accounts for at least 80% of total nitrogen excretion (Braun *et al*, 2009a). Whether the significant reduction in ammonia excretion caused by AQP1a knockdown results in a corresponding increase in nitrogen excretion as urea remains to be determined. Such an effect could account for the apparent lack of ammonia accumulation in the

tissues of AQP1a morphant larvae, as would be expected if ammonia excretion *via* AQP1a were reduced in the absence of any compensatory mechanism. To our knowledge, the present study is the first to examine the contribution of AQP1a to nitrogenous waste excretion in teleost fish. Studies that assess the physiological role AQP1a or other AQP isoforms play in ammonia transport remain sparse. Three wheat AQPs, when expressed in a yeast mutant deficient in ammonium (NH_4^+) transport, were able to restore normal ammonia uptake (Jahn *et al*, 2004). Voltage clamp studies using mammalian AQP1-expressing lipid bilayers, however, contradicted these findings and suggested that AQP1 could not transport ammonia (Saparov *et al*, 2007). As with CO_2, the route taken by ammonia through AQP1a remains uncertain. It has been hypothesized that AQP1 transports electroneutral NH_3 instead of NH_4^+, and because NH_3 is a hydrophilic molecule it is expected, like water, to move exclusively through the AQP1 monomers (Musa-Aziz *et al*, 2009).

Emphasis has been placed on the role that the Rh glycoprotein family plays in ammonia excretion in zebrafish larvae (Nakada *et al*, 2007; Braun *et al*, 2009a). The Rh glycoprotein isoforms Rhag, Rhbg, and Rhcg1 are understood to be selective ammonia transporters (Nakada *et al*, 2007; Wright and Wood, 2009; Braun *et al*, 2009a). An approximately 50% reduction in J_{amm} was reported by Braun *et al* (2009a) upon knockdown of any of these three isoforms in larvae. Both AQP1a and Rhcg1 are located in the HR cells of the larval yolk sac epithelium (Nakada *et al*, 2007; Kwong *et al*, 2013), where they are well-placed to facilitate ammonia excretion. The elevated capacity of the HR cells to excrete protons likely also contributes to ammonia efflux *via* the "acid-trapping" mechanism. Ammonia exits the apical membrane of HR cells *via* Rhcg1, and encounters H^+ extruded by H^+-ATPase, allowing it to be protonated to NH_4^+; this effect maintains the outwardly-directed NH_3 gradient necessary for excretion (Wright

and Wood, 2009). The relative contributions of AQP1a and Rhcg1 to ammonia excretion remain to be determined. To gain insight into the proportion of ammonia excretion *via* AQP1a *versus* Rhcg1, double knockdown studies could be performed. Using morpholino oligonucleotides targeted to AQP1a and Rhcg1, ammonia excretion in AQP1a/Rhcg1 double morphants could be assessed relative to rates in single AQP1a or Rhcg1 morphants.

4.4 AQP1a on the yolk sac epithelium is important for gas excretion

The tissue localization of AQP1a appears to change over the course of zebrafish embryogenesis and larval development. From 72 hpf, Chen *et al* (2010) reported abundant AQP1a mRNA expression on the yolk sac epithelium, in what were later found by immunohistochemistry and confocal microscopy to be two subtypes of ionocytes; HR cells and NaR cells (Kwong *et al*, 2013). The presence of AQP1 in the plasma membrane of RBCs was well-documented in humans (Endeward *et al,* 2006). In zebrafish larvae, AQP1a expression was localized by *in situ* hybridization to the RBC from 48 hpf (Chen *et al* 2010) and at 96 hpf by immunohistochemistry (current study). The expression of AQP1a also has been observed in vascular endothelial cells in 4 dpf larvae (Chen *et al*, 2010; Rehn *et al*, 2011). We therefore asked the following question; at which one (or more) of these locations in the larval zebrafish is AQP1a playing a role in gas excretion? In adult fish, RBCs and the gill epithelium both play important roles in CO_2 excretion (Perry and Gilmour, 2006), but during early development, the importance of RBCs in gas exchange is less clear-cut. The small size of embryos/larvae and the understanding that gas movement occurs largely cutaneously prior to the development of gills at 14 dpf – indeed, RBCs and gills are not required for O_2 uptake until two weeks post fertilization (Rombough, 2002) – led to the hypothesis that yolk sac epithelium AQP1a is the primary route through which CO_2 and ammonia will pass.

Phenylhydrazine (PHZ) is a haemolytic agent used experimentally to induce anaemia. Its use has been tested in several teleosts, including goldfish (Houston *et al*, 1988), rainbow trout (Gilmour and Perry, 1996), and zebrafish (Pelster and Burggren, 1996). Staining of PHZ-treated and control larvae with *o*-dianisidine, a haeme-specific dye (Detrich *et al*, 1995) confirmed the loss of RBCs in PHZ-treated zebrafish larvae. Loss of RBCs through PHZ-induced haemolysis should eliminate RBC AQP1a, leaving only the AQP1a on the yolk sac for excretory functions. If the contribution of RBC AQP1a to CO_2 and ammonia excretion is negligible, then whole-body $\dot{M}CO_2$ and *RER* (as well as J_{amm}) should not change following treatment of larvae with PHZ. Indeed, this result was observed and because AQP1a knockdown continued to decrease CO_2 excretion in the RBC-deficient larvae, RBC AQP1a can be eliminated as a site of CO_2 excretion, confirming yolk sac AQP1a as the key site of CO_2 excretion in larval zebrafish.

Although the significant reduction in CO_2 excretion in AQP1a morphant larvae was apparent following application of PHZ, AQP1a morphants in this experimental series exhibited a significant reduction in metabolic rate (measured as O_2 uptake, $\dot{M}O_2$). This result was in contrast to the initial experimental series using AQP1a knockdown, where a specific effect on CO_2 excretion but not O_2 uptake was detected. The reason for this difference between experimental series was not obvious. Notably, however, whereas the $\dot{M}O_2$ values measured for these larvae were comparable to those reported previously for 4 dpf zebrafish larvae (Gilmour *et al* 2009), the absolute $\dot{M}CO_2$ values observed in this experiment (10-22 μmol g^{-1} h^{-1}) were substantially lower than those measured in the initial experimental series or those reported by Gilmour *et al* (2009) for 4 dpf zebrafish (~55 μmol g^{-1} h^{-1}), resulting in *RER* values that were unrealistically low. Despite these concerns, the magnitude of the fall in $\dot{M}O_2$ was smaller than the magnitude of the reduction in $\dot{M}CO_2$; thus *RER* was reduced in the morphants subjected to PHZ treatment

indicating that at least part of the effect on CO_2 excretion could still be attributed to the translational knockdown of AQP1a.

The results of this series of experiments were particularly interesting because they implied that RBCs are not necessary for either O_2 uptake or CO_2 excretion in developing zebrafish. Pelster and Burggren (1996) reported that PHZ-induced haemolysis did not impact O_2 consumption or cardiac performance in larval zebrafish. Similar results indicating that the RBC is not necessary for O_2 uptake at the early stages of development in fish were reported by others (e.g. Weinstein *et al*, 1996; Rombough, 2002; Rombough and Drader, 2009). However, inhibition of CA by acetazolamide decreased $\dot{M}CO_2$ significantly compared to controls in 48 hpf zebrafish larvae (Gilmour *et al*, 2009), as did selective translational knockdown of RBC CA (zCAb; Gilmour *et al*, 2009). These results imply a role for the RBC in CO_2 excretion at 48 hpf and therefore are in opposition to what was observed in the present study in 4 dpf larvae. Resolving this apparent discrepancy will require additional work.

4.5 Rhcg1 knockdown does not promote AQP1a expression (and *vice versa*)

The contribution of AQP1a to CO_2 excretion in zebrafish relative to simple diffusion of CO_2 through membranes and/or movement of CO_2 through Rh glycoproteins (Perry *et al*, 2010) remains an open question. Simulations of molecular dynamics have suggested that the free energy barrier for CO_2 permeation *via* AQP1 is higher than that for the lipid bilayer (Hub and de Groot, 2006); thus, the AQP1 contribution to CO_2 movement might only be physiologically relevant for membranes with intrinsically low CO_2 permeability. It is tempting to speculate, however, that in membranes where AQP1a is abundantly expressed (such as the HR and NaR ionocytes of the larval zebrafish yolk sac epithelium), the contribution of AQP1a to

transmembrane CO_2 permeability has the potential to be significant. The human RBC membrane, for example, carries ~140 000 copies of AQP1 (Wang *et al*, 2007) and AQP1 makes a significant contribution to CO_2 transfer in this system (Endeward *et al*, 2006). The most substantial knockdown observed in the present study (~80% less AQP1a protein abundance relative to sham-injected larvae) reduced $\dot{M}CO_2$ by approximately one-third, suggesting the potential for AQP1a to make a significant contribution to CO_2 movement.

Rhcg1 is understood to be a multi-functional transporter of CO_2 and ammonia in larval zebrafish (Perry *et al*, 2010), and its co-localization with AQP1a in the HR cells of the yolk sac epithelium (Kwong *et al,* 2013) lends credence to the hypothesis that the two channels might act in concert *vis-à-vis* CO_2 and ammonia transfer. However, knockdown of one of these gas channels did not result in a significant increase in the mRNA or protein expression of the other gas channel. Some work suggests that AQP1a is expressed in the basolateral membrane of HR cells (Kwong *et al*, 2013), whereas Rhcg1 exhibits an apical localization (Nakada *et al*, 2007), and different cellular patterns of protein localization would presumably reduce the likelihood of interaction between these gas channels. However, because only partial reduction of the expression of either gas channel was achieved (on average an ~50% decrease in protein expression compared to sham-injected larvae), it is also possible that the stimulus for upregulation of the expression of AQP1a in the reduced presence of Rhcg1 (and *vice versa*) in the ionocytes of the yolk sac might not have been sufficient. Application of a strong inhibitor of AQP1a or use of an AQP1a knock*out* model could perhaps shed more light on the possibility of interactions between AQP1a and Rhcg1 with respect to CO_2 excretion.

4.6 HEA challenge increased AQP1a expression in Rhcg1 morphants

Having characterized zebrafish AQP1a as a multi-functional transporter of both CO_2 and ammonia, an obvious next step was to determine whether AQP1a expression was modulated in response to environmental conditions that challenged ammonia excretion. The first condition examined was HEA, because Braun *et al* (2009b) demonstrated that HEA (500 μM NH_4Cl, the condition used in the present study) significantly reduced ammonia excretion in 4 dpf zebrafish larvae, resulting in accumulation of tissue ammonia levels and compensatory increases in Rhag and Rhcg1 mRNA expression. Presumably, upregulation of these ammonia transporters occurred to enhance the capacity for ammonia excretion (Braun *et al,* 2009b). Given the role that AQP1a can play in ammonia excretion in developing zebrafish, HEA challenge would be predicted to trigger an increase in AQP1a mRNA and protein expression.

Chronic exposure of wild-type larvae to HEA did not affect AQP1a mRNA or protein abundance significantly. These results and the prior work by Braun *et al* (2009b) suggested that there is sufficient capacity for elevated ammonia excretion under conditions of HEA within the Rh glycoprotein family. Elimination of Rhcg1 (or at least a significant reduction in Rhcg1 expression) *via* translational knockdown could potentially shift the need for elevated ammonia excretion onto alternative pathways, such as AQP1a as an ammonia transporter. In accordance with this prediction, Rhcg1 morphants exposed to HEA were found to express significantly higher levels of AQP1a protein compared to sham-injected larvae. Thus, in the presence of constraints on Rhcg1 expression, AQP1a was upregulated in a secondary manner to enhance ammonia excretion.

4.7 Exposure to pH 10 water reduced AQP1a protein expression

Normal ammonia efflux requires available free protons in the external environment so that NH_3 may be protonated to NH_4^+ at the cell boundary layer, thereby maintaining the outwardly-directed NH_3 partial pressure gradient (Wright and Wood, 2009). Impairment of this "acid-trapping" mechanism of ammonia excretion can be achieved by exposure of the fish to high pH conditions. The Lake Magadi tilapia (*Alcolapia graham*) is, perhaps, the most extreme example of this effect – it is an obligate ureotele owing to the high pH (~9.6-10) of its environment (Randall *et al,* 1989; Wood *et al,* 1989). Exposure of (adult) fish of other species to alkaline water typically results in an initial inhibition of ammonia excretion, followed by recovery of ammonia excretion as blood total ammonia levels rise to re-establish the NH_3 partial pressure gradient (e.g. Wilkie and Wood, 1991; Yesaki and Iwama, 1992; Wilkie and Wood, 1995; Wilkie *et al,* 1996). In 5 dpf zebrafish larvae, Shih *et al* (2008) demonstrated that the NH_4^+ gradient close to the yolk sac epithelium decreased with increasing external pH, a finding that was corroborated in the present study by the measurement of a significant reduction in ammonia excretion in 4 dpf wild-type zebrafish larvae acutely exposed to pH 10 water. Exposure to pH 10 water also would be predicted to enhance CO_2 excretion, because hydration of excreted CO_2 in the boundary layer helps to maintain the partial pressure gradient for CO_2 excretion and this acid-generating reaction would be favoured under conditions of high pH. Although measurements of CO_2 excretion in high pH water appear to be lacking from the literature, several studies have documented a fall in the partial pressure of CO_2 in the blood of (adult) fish exposed to high pH, a response that is consistent with enhancement of CO_2 excretion (e.g. Thomas and Poupin, 1985; Wilkie *et al*, 1994; Wilkie and Wood, 1995; Wilkie *et al*, 1996). However, neither absolute $\dot{M}CO_2$ nor *RER* decreased following acute exposure of 4 dpf zebrafish larvae to pH 10 water in the present study. Reduction of ammonia excretion by exposure to pH

10 water would be expected to be accompanied by the accumulation of ammonia in the tissues, and as with HEA, upregulation of AQP1a in its role as an ammonia transporter would be predicted to help to alleviate this problem. In contrast to this prediction, however, exposure to pH 10 water caused a marked and significant reduction in the expression of AQP1a protein, in both wild-type larvae and Rhcg1 morphants. This result suggests that AQP1a protein levels responded to an effect of pH 10 exposure other than the inhibition of ammonia excretion. The trigger responsible for this effect, however, remains to be identified.

4.8 Summary and perspectives

Freshwater teleosts, by virtue of being hyper-osmotic to their environment, face the challenge of constant osmotic influx of water. As such, the presence of AQP1a on the larval zebrafish yolk sac epithelium is puzzling – attempts to limit water influx (for example, by limiting AQP1a expression in the integument) would instead be expected. Perhaps, then, expression of AQP1a on the larval body surface is driven by something other than osmoregulatory requirements. Whereas previous *in vitro* studies had identified AQP1a as a potential conductor of both CO_2 and ammonia, the results of the present study are the first to confirm that AQP1a plays a physiologically-relevant role in CO_2 and nitrogenous waste excretion in teleost fish. Indeed, the present study is the first to investigate *in vivo* a physiological role for AQPs in teleosts beyond osmoregulation. Using larval zebrafish as the study species, AQP1a was found to be a selective transporter of both CO_2 and ammonia; knockdown of this multi-functional gas channel significantly reduced whole-larva rates of CO_2 and ammonia excretion. In the face of environmental stressors that impair ammonia excretion, such as HEA or high pH, expression of AQP1a was modulated.

In summary, two classes of multi-functional gas channels now are known to exist in zebrafish; AQPs and Rh glycoproteins. Moving forward, it would be of interest to further examine potential interactions between members of these two families. Although the results of the present study did not conclusively link AQP1a and Rhcg1 expression and function, many avenues for exploration remain. The exact route of gas conduction through AQP1a also remains an open question, and the dynamics of AQP1a expression under other physiologically-challenging conditions (such as exercise) should be explored. Finally, AQP1a is but one of multiple possible AQPs that could be important to gas exchange in teleosts. Exploration of these additional candidates awaits future research.

5. REFERENCES

Agre, P., Preston, G. M., Smith, B. L., Jung, J. S., Raina, S., Moon, C. and Nielsen, S. (1993). Aquaporin CHIP: the archetypal molecular water channel. *Am. J. Physiol.*, **265**, F463–76.

Beitz, E., Wu, B., Holm, L. M., Schultz, J. E. and Zeuthen, T. (2006). Point mutations in the aromatic/arginine region in aquaporin 1 allow passage of urea, glycerol, ammonia, and protons. *PNAS*, **103**(2), 269–74.

Bill, B. R., Petzold, A. M., Clark, K. J., Schimmenti, L. A. and Ekker, S. C. (2009). A primer for morpholino use in zebrafish. *Zebrafish*, **6**(1), 69–77.

Boron, W. F. (2010). Sharpey-Schafer lecture: gas channels. *Exp. Physiol.*, **95**(12), 1107-30.

Boron, W. F. (2006). Acid-base transport by the renal proximal tubule. *J. Am. Soc. Nephrol.,* **17**(9), 2368–82.

Boutilier, R. G., Heming, T. A. and Iwama, G. K. (1984). Physicochemical parameters for use in fish respiratory physiology. *In* Fish physiology, Vol. X. *Edited by* Hoar, W. S., and Randall, D. J. Academic Press, New York, pp. 403-30.

Braun, M. H., Steele, S. L., Ekker, M. and Perry, S. F. (2009a). Nitrogen excretion in developing zebrafish (*Danio rerio*): a role for Rh proteins and urea transporters. *Am. J. Physiol.,* **296**(5), F994-1005.

Braun, M. H., Steele, S. L. and Perry, S. F. (2009b). The responses of zebrafish (*Danio rerio*) to high external ammonia and urea transporter inhibition: nitrogen excretion and expression of rhesus glycoproteins and urea transporter proteins. *J. Exp. Biol.*, **212**(23), 3846-56.

Cameron, J. N. (1976). Branchial ion uptake in arctic grayling: resting values and effects of acid-base disturbance. *J. Exp. Biol.*, **64**(3), 711–25.

Carlsson, O., Nielsen, S., Zakaria el-R and Rippe, B. (1996). *In vivo* inhibition of transcellular water channels (aquaporin-1) during acute peritoneal dialysis in rats. *Am. J. Physiol*, **271**, H2254-62.

Cerdà, J. and Finn, R. N. (2010). Piscine aquaporins: an overview of recent advances. *J. Exp. Zool.*, **313**(10), 623-50.

Chadwick, T. and Wright, P. (1999). Nitrogen excretion and expression of urea cycle enzymes in the Atlantic cod (*Gadus morhua l.*): a comparison of early life stages with adults. *J. Exp. Biol.*, **202**, 2653–62.

Chen, L.-M., Zhao, J., Musa-Aziz, R., Pelletier, M. F., Drummond, I. A. and Boron, W. F. (2010). Cloning and characterization of a zebrafish homologue of human AQP1: a bifunctional water and gas channel. *Am. J. Physiol.*, **299**(5), R1163-74.

Cherif-Zahar, B., Durand, A., Schmidt, I., Hamdaoui, N., Matic, I., Merrick, M. and Matassi, G. (2007). Evolution and functional characterization of the RH50 gene from the ammonia-oxidizing bacterium *Nitrosomonas europaea*. *J. Bacteriol.*, **189**(24), 9090–100.

Cooper, G. J. and Boron, W. F. (1998). Effect of PCMBS on CO_2 permeability of Xenopus oocytes expressing aquaporin 1 or its C189S mutant. *Am. J. Physiol.*, **275**, C1481-6.

Cooper, G. J., Zhou, Y., Bouyer, P., Grichtchenko, I. I. and Boron, W. F. (2002). Transport of volatile solutes through AQP1. *J. Physiol.*, **542**(1), 17–29.

de Groot, B. L. and Grubmüller, H. (2005) The dynamics and energetics of water permeation and proton exclusion in aquaporins. *Curr. Opin. Struct. Biol.,* **15,** 176–83

Detrich, H. W., Kieran, M. W., Chan, F. Y., Barone, L. M., Yee, K., Rundstadler, J. A, Pratt, S., Ransom, D. and Zon, L. I. (1995). Intraembryonic hematopoietic cell migration during vertebrate development. *PNAS*, **92**(23), 10713-7.

Endeward, V., Cartron, J.-P., Ripoche, P. and Gros, G. (2008). RhAG protein of the Rhesus complex is a CO_2 channel in the human red cell membrane. *FASEB*, **22**(1), 64-73.

Fang, X., Yang, B., Matthay, M. A. and Verkman, A. S. (2002). Evidence against aquaporin-1-dependent CO_2 permeability in lung and kidney. *J. Physiol.*, **542**(1), 63–9.

Gilmour, K. M. and Perry, S. F. (1996). The effects of experimental anaemia on CO_2 excretion *in vitro* in rainbow trout, *Oncorhynchus mykiss*. *Fish Physiol. Biochem.*, **15**(1), 83-94.

Gilmour, K. M., Thomas, K., Esbaugh, A. J. and Perry, S. F. (2009). Carbonic anhydrase expression and CO_2 excretion during early development in zebrafish *Danio rerio*. *J. Exp. Biol.*, **212**, 3837-45.

Hamdi, M., Sanchez, M. A., Beene, L. C., Liu, Q., Landfear, S. M., Rosen, B. P. and Liu, Z. (2009). Arsenic transport by zebrafish aquaglyceroporins. *BMC Mol. Biol.*, **10**, 104.

Herrera, M., Hong, N. J. and Garvin, J. L. (2006). Aquaporin-1 transports NO across cell membranes. *Hypertension*, **48**(1), 157-64.

Holm, L. M., Jahn, T. P., Møller, A. L. B., Schjoerring, J. K., Ferri, D., Klaerke, D. A. and Zeuthen, T. (2005). NH_3 and NH_4^+ permeability in aquaporin-expressing *Xenopus* oocytes. *Eur. J. Physiol.*, **450**(6), 415–28.

Houston, A. H., Murad, A. and Gray, J. D. (1988). Induction of anemia in goldfish, *Carassius auratus L.*, by immersion in phenylhydrazine hydrochloride. *Can. J. Zool.*, 66, 729-36.

Hub, J. S. and de Groot, B. L. (2006). Does CO_2 permeate through aquaporin-1? *Biophys. J.*, **91**(3), 842–8.

Jahn T. P., Moller A. L., Zeuthen T., Holm L. M., Klaerke D. A., Mohsin B., Kühlbrandt, W. and Schjoerring, J. K. (2004). Aquaporin homologues in plants and mammals transport ammonia. *FEBS Lett.*, **574,** 31–6.

Kumai, Y. and Perry, S. F. (2011). Ammonia excretion *via* Rhcg1 facilitates Na^+ uptake in larval zebrafish, *Danio rerio*, in acidic water. *Am. J. Physiol.,* **301**, 1517–28.

Kustu, S. and Inwood, W. (2006). Biological gas channels for NH_3 and CO_2: evidence that Rh (Rhesus) proteins are CO_2 channels. *Transfusion clinique et biologique*, **13**(1-2), 103-10.

Kwong, R. W. M., Kumai, Y. and Perry, S. F. (2013). The role of aquaporin and tight junction proteins in the regulation of water movement in larval zebrafish (*Danio rerio*). *PloS One*, **8**(8), e70764.

Liakopoulos, V., Zarogiannis, S., Hatzoglou, C., Kourti, P., Poultsidi, A., Eleftheriadis, T., Gourgoulianis, K., Molyvdas, P.-A. and Stefanidis, I. (2006). Inhibition by mercuric chloride of aquaporin-1 in the parietal sheep peritoneum: an electrophysiologic study. *Adv. Peritoneal. Dialysis*, **22**, 7-10.

Marchissio, M. J., Francés, D. E. A., Carnovale, C. E. and Marinelli, R. A. (2012). Mitochondrial aquaporin-8 knockdown in human hepatoma HepG2 cells causes ROS-induced mitochondrial depolarization and loss of *via*bility. *Toxicol. Appl. Pharmacol.*, **264**(2), 246–54.

Musa-Aziz, R., Chen, L.-M., Pelletier, M. F. and Boron, W. F. (2009). Relative CO_2/NH_3 selectivities of AQP1, AQP4, AQP5, AmtB, and RhAG. *PNAS*, **106**(13), 5406-11.

Nakada, T., Hoshijima, K., Esaki, M., Nagayoshi, S., Kawakami, K. and Hirose, S. (2007). Localization of ammonia transporter Rhcg1 in mitochondrion-rich cells of yolk sac, gill, and kidney of zebrafish and its ionic strength-dependent expression. *Am. J. Physiol.*, **293**, 1743–53.

Nahkoul, N. L., Davis, B. A., Romero, M. F. and Boron, W. F. (1998). Effect of expressing the water channel aquaporin-1 on the CO_2 permeability of *Xenopus* oocytes. *Am. Physiol. Soc.*, **274**, 543–48.

Nakhoul, N. L., Hering-Smith, K. S., Abdulnour-Nakhoul, S. M. and Lee, L. (2001). Transport of NH_3/NH_4^+ in oocytes expressing aquaporin-1. *Am. J. Physiol.,* **281**, F255-63.

Pellegrino, E. D. and Biltz, R. M. (1965). Bone carbonate and the Ca to P molar ratio. *Nature,* **219**, 1261-62.

Pelster, B. and Burggren, W. W. (1996). Disruption of hemoglobin oxygen transport does not impact oxygen-dependent physiological processes in developing embryos of zebrafish. *Circ. Res.*, **79**, 358-62.

Perry, S. F. (1986). Carbon dioxide excretion in fishes. *Can. J. Zool.*, **64**, 565–72.

Perry, S. F. and Gilmour, K. M. (2006). Acid-base balance and CO_2 excretion in fish: unanswered questions and emerging models. *Resp. Physiol. Neurobiol.*, **154**(1-2), 199–215.

Perry, S. F., Shahsavarani, A., Georgalis, T., Bayaa, M., Furimsky, M. and Thomas, S. L. Y. (2003). Channels, pumps, and exchangers in the gill and kidney of freshwater fishes: their role in ionic and acid-base regulation. *J. Exp. Biol.*, **300**(1), 53–62.

Perry, S. F., Braun, M. H., Noland, M., Dawdy, J. and Walsh, P. J. (2010). Do zebrafish Rh proteins act as dual ammonia-CO_2 channels? *J. Exp. Zool.*, **313**(9), 618-21.

Pfaffl, M. W. (2001). A new mathematical model for relative quantification in real-time RT-PCR. *Nucleic Acids Res.,* **29**, e45.

Pörtner, H. O., Boutilier, R. G., Tang, Y. and Toews, D. P. (1990). Determination of intracellular pH and P_{CO2} after metabolic inhibition by fluoride and nitrilotriacetic acid. *Resp. Physiol.*, **81**, 255–274.

Prasad, G. V., Coury, L. a, Finn, F. and Zeidel, M. L. (1998). Reconstituted aquaporin 1 water channels transport CO_2 across membranes. *J. Biol. Chem.*, **273**(50), 33123-6.

Randall, D., Wood, C., Perry, S., Bergman, H., Maloiy, G., Mommsen, T. and Wright, P. (1989). Urea excretion as a strategy for survival in a fish living in a very alkaline environment. *Nature*, **337**, 165–166.

Rehn, K., Wong, K. S., Balciunas, D. and Sumanas, S. (2011). Zebrafish enhancer trap line recapitulates embryonic aquaporin 1a expression pattern in vascular endothelial cells. *Int. J. Dev. Biol.*, **55**(6), 613–8.

Ripoche, P., Goossens, D., Devuyst, O., Gane, P., Colin, Y., Verkman, A. S. and Cartron, J.-P. (2006). Role of RhAG and AQP1 in NH_3 and CO_2 gas transport in red cell ghosts: a stopped-flow analysis. *Transf. Clin. Biol.*, **13**(1-2), 117-22.

Rombough, P. (2002). Gills are needed for ionoregulation before they are needed for O_2 uptake in developing zebrafish, *Danio rerio*. *J. Exp. Biol*, **205**(12), 1787-94.

Rombough, P. and Drader, H. (2009). Hemoglobin enhances oxygen uptake in larval zebrafish (*Danio rerio*) but only under conditions of extreme hypoxia. *J. Exp. Biol.*, **212**, 778–84.

Saparov, S. M., Liu, K., Agre, P. and Pohl, P. (2007). Fast and selective ammonia transport by aquaporin-8. *J. Biol. Chem.*, **282**(8), 5296–301.

Shih, T.-H., Horng, J.-L., Hwang, P.-P. and Lin, L.-Y. (2008). Ammonia excretion by the skin of zebrafish (*Danio rerio*) larvae. *Am. J. Physiol.*, **295**(6), C1625-32.

Singh, S. K., Binder, H. J., Geibel, J. P. and Boron, W. F. (1995). An apical permeability barrier to NH_3/NH_4^+ in isolated, perfused colonic crypts. *PNAS*, **92**(25), 11573–7.

Smith, P. K., Krohn, R. I., Hermanson, G. T., Mallia, A. K., Gartner, F. H., Provenzano, M. D. and Klenk, D. C. (1985). Measurement of protein using bicinchoninic acid. *Anal. Biochem.*, **150**, 76–85.

Thomas, S. and Poupin, J. (1985). A study of the effects of water carbonate alkalinity on some parameters of blood acid-base status in rainbow trout (*Salmo gairdneri* R.). *J. Comp. Physiol. B*, **2**, 29–34.

Tingaud-Sequeira, A., Calusinska, M., Finn, R. N., Chauvigné, F., Lozano, J. and Cerdà, J. (2010). The zebrafish genome encodes the largest vertebrate repertoire of functional aquaporins with dual paralogy and substrate specificities similar to mammals. *BMC Evol. Biol.*, **10**, 38.

Uehlein, N., Lovisolo, C., Siefritz, F. and Kaldenhoff, R. (2003). The tobacco aquaporin NtAQP1 is a membrane CO_2 pore with physiological functions. *Nature*, **425**(6959), 734–7.

Verbavatz, J. M., Brown, D., Sabolić, I., Valenti, G., Ausiello, D. A, Van Hoek, A. N., Ma, T. and Verkman, A. S. (1993). Tetrameric assembly of CHIP28 water channels in liposomes and cell membranes: a freeze-fracture study. *J. Cell Biol.*, **123**(3), 605–18.

Verdouw H., Van Echted C. J. A. and Dekkers E. M. J. (1978). Ammonia determination based on indophenol formation with sodium salicylate. *Water Res.*, **12,** 399–402.

Walz, T., Fujiyoshi, Y. and Engel, A. (2009). The AQP structure and functional implications. *Handbook Exp. Pharmacol.*, (190), 31–56.

Wang, Y., Cohen, J., Boron, W. F., Schulten, K. and Tajkhorshid, E. (2007). Exploring gas permeability of cellular membranes and membrane channels with molecular dynamics. *J. Struc. Biol.*, **157**(3), 534-44.

Weinstein, B. M., Schier, a F., Abdelilah, S., Malicki, J., Solnica-Krezel, L., Stemple, D. L., Stainier, D. Y., Zwartkruis, F., Driever, W. and Fishman, M. C. (1996). Hematopoietic mutations in the zebrafish. *Dev.*, **123**, 303–9.

Westerfield, M. (1993). The Zebrafish Book. Eugene, OR: University of Oregon Press.

Wilkie, M. P. (2002). Ammonia excretion and urea handling by fish gills: present understanding and future research challenges. *J. Exp. Zool.*, **293**(3), 284–301.

Wilkie, M. P. and Wood, C. M. (1991). Nitrogenous waste excretion, acid-base regulation, and ionoregulation in rainbow trout (*Oncorhynchus mykiss*) exposed to extremely alkaline water. *Physiol. Zool.*, **64**(4), 1069–86.

Wilkie, M. P., Wright, P. A., Iwama, G. K. and Wood, C. M. (1994). The physiological adaptations of the Lahontan cutthroat trout (*Oncorhynchus clarki henshawi*) following transfer

from well water to the highly alkaline waters of Pyramid Lake, Nevada (pH 9.4). *Physiol. Zool.*, **67**(2), 355–80.

Wilkie, M. P. and Wood, C. M. (1995). Recovery from high pH exposure in the rainbow trout: white muscle ammonia storage, ammonia washout, and the restoration of blood chemistry. *Physiol. Zool.*, **68**(3), 379–401.

Wilkie, M. P., Simmons, H. E. and Wood, C. M. (1996). Physiological adaptations of rainbow trout to chronically elevated water pH (pH = 9.5). *J. Exp. Biol.*, **274**(1), 1–14.

Wood, C. M., Perry, S. F., Wright, P. A, Bergman, H. L. and Randall, D. J. (1989). Ammonia and urea dynamics in the Lake Magadi tilapia, a ureotelic teleost fish adapted to an extremely alkaline environment. *Respir. Physiol.*, **77**(1), 1–20.

Wright, P., Felskie, A. and Anderson, P. (1995). Induction of ornithine-urea cycle enzymes and nitrogen metabolism and excretion in rainbow trout (*Oncorhynchus mykiss*) during early life stages. *J. Exp. Biol.*, **198**, 127-35.

Wright, P. A and W**ood, C. M.** (2009). A new paradigm for ammonia excretion in aquatic animals: role of Rhesus (Rh) glycoproteins. *J. Exp. Biol.*, **212**, 2303-12.

Wu, B. and Beitz, E. (2007). Aquaporins with selectivity for unconventional permeants. *Cell. Molec. Life Sci.*, **64**(18), 2413–21.

Yang, B., Fukuda, N., van Hoek, A. N., Matthaw, M. A., Ma, T. and Verkman, A. S. (2000). Carbon dioxide permeability of aquaporin-1 measured in erythrocytes and lung of aquaporin-1 null mice and in reconstituted proteoliposomes. *J. Biol. Chem.*, **275**(4), 2686–92.

Yesaki, T. and Iwama, G. (1992). Survival, acid-base regulation, ion regulation, and ammonia excretion in rainbow trout in highly alkaline hard water. *Physiol. Zool*., **65**, 763–787.

Yukutake, Y., Tsuji, S., Hirano, Y., Adachi, T., Takahashi, T., Fujihara, K., Agre, P., Yasui M. and Suematsu, M. (2008). Mercury chloride decreases the water permeability of aquaporin-4-reconstituted proteoliposomes. *Biol. Cell.*, **100**(6), 355-63.